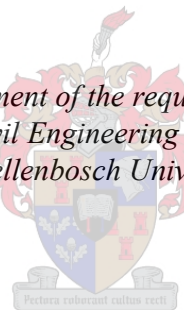


# **Comparison of 2D and 3D slope stability factors of safety considering spatial variability**

by  
Tawanda Blessing Mutede

*Thesis presented in fulfilment of the requirements for the degree of  
Master of Engineering in Civil Engineering in the Faculty of Engineering  
at Stellenbosch University*



Supervisor: Dr Charles MacRobert

April 2022

## Plagiaatverklaring / Plagiarism Declaration

- 1 Plagiaat is die oorneem en gebruik van die idees, materiaal en ander intellektuele eiendom van ander persone asof dit jou eie werk is.

*Plagiarism is using ideas, material and other intellectual property of another's work and presenting it as my own.*

- 2 Ek erken dat die pleeg van plagiaat 'n strafbare oortreding is aangesien dit 'n vorm van diefstal is.

*I agree that plagiarism is a punishable offence because it constitutes theft.*

- 3 Ek verstaan ook dat direkte vertalings plagiaat is.

I also understand that direct translations are plagiarism.

- 4 Dienooreenkomsdig is alle aanhalings en bydraes vanuit enige bron (ingesluit die internet) volledig verwys (erken). Ek erken dat die woordelikse aanhaal van teks sonder aanhalingstekens (selfs al word die bron volledig erken) plagiaat is.

*Accordingly, all quotations and contributions from any source whatsoever (including the internet) have been cited fully. I understand that the reproduction of text without quotation marks (even when the source is cited) is plagiarism.*

- 5 Ek verklaar dat die werk in hierdie skryfstuk vervat, behalwe waar anders aangedui, my eie oorspronklike werk is en dat ek dit nie vantevore in die geheel, of gedeeltelik, ingehandig het om enige kwaifikasie te verwerf nie.

*I declare that the work contained in this thesis/dissertation, except where otherwise stated, is my original work, and that I have not previously in its entirety, or in part, submitted this thesis/dissertation to obtain any qualification.*

## Abstract

Historically, slope stability analyses have relied on two-dimensional (2D) models. This is due to the relative ease of implementing 2D slope stability analysis both from a theoretical and computational stand-point. However, with the emergence of powerful computers, the use of three-dimensional (3D) methods is increasing. While 3D slope stability analysis methods model reality better, site investigation methods often do not provide adequate information to create detailed 3D slope models. As a result, the extrapolation of 2D cross sections to generate 3D models is employed. This simplification gives rise to the question of whether these 3D extrapolated analyses are safe, as this typically results in higher factors of safety compared to the corresponding 2D analyses. Extrapolation may hide the spatial variability along slopes leading to an unsafe analysis.

This research aimed to determine whether it was safe to conduct 3D slope stability simulations using extrapolated 2D sections or whether it was safer to analyse slopes using simple 2D methods. This research was done with reference to tailings dams. A total of 816 different slopes were generated and analysed using Rocscience's Slide 2 and Slide 3 software programs. Three different models were used to conduct slope stability analyses, namely: 2D models, 3D extrapolated models from 2D extrapolated sections and 3D composite models which consisted of three merged 2D extrapolated slope sections.

The research found that when analysing slopes, if the weakest slope sections are sampled and analysed using 3D extrapolated models, the results that are obtained are safe. However, if the strongest slope section is unfortunately sampled and analysed using 3D extrapolated models, the results obtained are unsafe. In such instances it is safer to rely on normal 2D modelling for analysis of slopes. The reason for this is that 3D extrapolated models' factor of safety (FOS) do not consider heterogeneity along a slope.

With relation to tailings dams, the research concluded that unless extensive sampling is done during the site investigation phase, it is safer to rely on 2D slope stability results especially when the tailings dam has thin embankment walls and high levels of heterogeneity. If good sampling procedures are done during the soil investigation phase, chances of identifying the weak and critical slope sections are increased. This makes the extrapolation of 2D slopes to conduct 3D slope stability analysis safer.

## **Opsomming**

Histories het hellingstabiliteitsontledings staatgemaak op tweedimensionele (2D) modelle. Dit is te wyte aan die relatiewe gemak van die implementering van 2D-hellingstabiliteitsanalise vanuit 'n teoretiese en berekeningsoogpunt. Met die opkoms van kragtige rekenaars, neem die gebruik van driedimensionele (3D) metodes toe. Alhoewel 3D-hellingstabiliteitsanaliseringsmetodes die werklikheid beter weerspieël, bied werfondersoekmetodes dikwels nie voldoende inligting om gedetailleerde 3D-hellingmodelle te skep nie. As gevolg hiervan word die ekstrapolasie van 2D-dwarssnitte gebruik om 3D-modelle te genereer. Hierdie vereenvoudiging laat die vraag ontstaan of hierdie 3D-geëkstrapoleerde ontledings veilig is, aangesien dit gewoonlik hoër veiligheidsfaktore in vergelyking met die ooreenstemmende 2D-ontledings tot gevolg het. Ekstrapolasie kan die ruimtelike veranderlikes van die hange verberg, wat tot 'n onveilige ontleding kan lei.

Hierdie navorsing was daarop gemik om vas te stel of dit veilig is om 3D-hellingstabiliteitsimulasies uit te voer met behulp van geëkstrapoleerde 2D-gedeeltes of dat dit veiliger is om hange te analyseer met behulp van eenvoudige 2D-metodes. Hierdie navorsing is gedoen met verwysing na uitskotdamme. 816 Verskillende hellings is gegenereer en ontleed met behulp van Rocscience's Slide 2 en Slide 3 sagteware programme. Drie verskillende modelle is gebruik om hellingstabiliteitsanalises uit te voer, naamlik: 2D-modelle, 3D-geëkstrapoleerde modelle van 2D-geëkstrapoleerde gedeeltes en 3D-saamgestelde modelle wat bestaan uit drie saamgevoegde 2D-geëkstrapoleerde hellingafdelings.

Navorsing het met ontleding van die hange bevind dat as die swakste hellingafdelings met behulp van 3D-geëkstrapoleerde modelle gemeet en ontleed word, die resultate veilig is. Maar wanneer monsters van die sterkste hellinggedeeltes ontleed word met behulp van 3D-geëkstrapoleerde modelle, is die resultate onveilige. In hierdie gevalle is dit veiliger om op normale 2D-modellering staat te maak vir die ontleding van hellings. Die rede hiervoor is dat 3D-geëkstrapoleerde modelle se "factor of safety" (FOS) nie heterogeniteit oor 'n helling in ag neem nie.

Met betrekking tot uitskotdamme, het die navorsing tot die gevolgtrekking gekom dat tensy uitgebreide monsterneming tydens die terreinondersoekfase gedoen word, dit veiliger is om op 2D-hellingstabiliteitsresultate staat te maak, veral as die uitskotdam dun damwalle en hoë heterogeniteit het. As goeie monsternemingsprosedures tydens die grondondersoekfase uitgevoer word, is die kans om die swak en kritieke hellinggedeeltes te identifiseer groter. Dit maak die ekstrapolasie van 2D-hange om 3D-hellingstabiliteitsanalise te doen, veiliger.

## **Dedication**

Firstly, I would like to dedicate this Thesis to Almighty God for giving me the strength and wisdom to reach this point. I would like to give special dedication to my parents and brother who supported me during my academic journey thus far. Furthermore, I want to dedicate this thesis to all my teachers and lectures from across the world, for the knowledge I have acquired which has helped me to this stage.

Glory be to God. We do our best and God will do the rest.

## Acknowledgements

I would like to acknowledge express my gratitude to Stellenbosch University for giving me the opportunity to do my thesis and Master's studies. I would also like to extend my gratitude to Dr C. MacRobert for continuously guiding me during my Master's study and for his plethora of knowledge, motivation and patience. His guidance has been of tremendous help in the research and writing of this thesis.

I would also like to thank my fellow colleagues who I have spent sleepless nights having stimulating discussions working on deadlines. Special thanks to Shane Teek for giving me a eureka moment during a particularly difficult planning stage of the research. I would like to give special thanks to the computer technicians at Stellenbosch University for organizing the necessary computers as well as installing the software which were needed for the execution of this research.

Lastly, I would like to my family: parents Mutandwa and Tandiwe Mutede and younger brother Tawana Mutede for their continuous guidance and ideas that have kept me persevering during my Master's studies.

## Table of contents

Abstract .....	iii
Opsomming .....	iv
Dedication .....	v
Acknowledgements .....	vi
Table of contents .....	vii
List of Tables.....	ix
List of figures .....	x
Abbreviations and symbols .....	xii
List of published papers .....	xiii
Chapter 1: Introduction .....	1
1.1 Background and Justification .....	1
1.2 Objectives and aims .....	2
1.3 Limitations and challenges.....	3
1.4 Report Structure .....	3
Chapter 2: Literature review.....	4
2.1 General .....	4
2.2 Tailings dams .....	4
2.3 Tailings dams site investigations.....	8
2.4 Slope stability analysis .....	10
2.5 Spatial variability .....	18
Chapter 3: Methodology.....	24
3.1 Introduction .....	24
3.2 Preliminary modelling.....	24
3.3 Study models .....	27
Chapter 4: Results, Analysis and Discussion .....	35
4.1 Introduction .....	35
4.2 Presentation of typical slip surfaces .....	35

4.3 Comparison of Analysis methods FOS results.....	38
4.4 Overall frequency screening of results.....	40
4.5 Analysis of the ideal and worst-case .....	44
4.6 Analysis using coefficient of variation.....	48
4.7 ANOVA Test.....	54
4.8 Findings and Practical implications .....	56
Chapter 5: Conclusion and recommendations .....	57
References .....	59
Annexure: A .....	62
Annexure B.....	65
Annexure C.....	71

## List of Tables

Table 2.1: Limit Equilibrium Methods (LEM) Summary Table (reproduced from Duncan et al. 2014) .....	12
Table 2.2: 2D Limit Equilibrium Methods Applications Summary Table (reproduced from Duncan et al. 2014) .....	13
Table 2.3: 3D Limit Equilibrium Methods (LEM) Summary Table (Aktahr, 2011) .....	15
Table 2.4: 2D vs 3D slope stability analysis comparisons .....	16
Table 2.5: Recommended factors of safety based on (ANCOLD, 2012) and (Anglo-American, 2019) and (ICOLD, 2020).....	17
Table 3.1: Outer Geometry Coordinates Table .....	24
Table 3.2: Trial-run internal boundary coordinates.....	25
Table 3.3: Preliminary Soil Properties .....	25
Table 3.4: Summary of soil parameters.....	28
Table 3.5: Varied Parameters .....	29
Table 3.6: Results obtained .....	32
Table 3.7: Simulation scenarios .....	32
Table 3.8: Study models initial summary.....	33
Table 4.1: Study models final summary.....	41
Table 4.2: Summarised 2D versus 3D comparison data .....	43
Table 4.3: Safety comparison for $F_{EXT}$ compared to $F_{COMP}$ .....	46
Table 4.4: Safety comparison for $F_{2D}$ compared to $F_{COMP}$ .....	48
Table 4.5: Low versus high spatial variability comparison.....	52
Table 4.6: Low versus high spatial variability comparison table.....	53
Table 4.7: Comparison of layering.....	55
Table 4.8: p values.....	55
Table A. 1: Excel Data record guide .....	62
Table B. 1: Simulation scenarios.....	65
Table B. 2: 2D slope analysis average data based on internal boundary thickness.....	68
Table B. 3: 3D Extrapolated slope analysis average data based on internal boundary thickness .....	69
Table B. 4: 3D Composite slope analysis average data based on internal boundary thickness .....	70

## List of figures

Figure 2.1: Upstream construction (Vick, 1990).....	5
Figure 2.2: Downstream construction (Vick, 1990).....	6
Figure 2.3: Centreline construction (Vick, 1990).....	6
Figure 2.4: Schematic of a typical tailings dam site investigation (Wei et al 2016).....	9
Figure 2.5: Slope cross section, sliding mass, slices and variables associated with each slice (Ranjan & Rao, 2000) .....	11
Figure 2.7: Tailings Dam cross section with typical beach illustration (Pan et al. 2017)....	18
Figure 3.1: Trial slope .....	25
Figure 3.2: Preliminary 2D model analysis result, Courtesy of Slide 2.....	26
Figure 3.3: Faulty preliminary 3D simulation result, Courtesy of Slide 3 .....	26
Figure 3.4: Sloped cross section with 5m stepped placement layer .....	27
Figure 3.5: Sloped cross section with 3.5 m stepped placement layer.....	27
Figure 3.6: Sloped cross section with 2.5 m stepped placement layer.....	28
Figure 3.7: Sloped cross section with 1.5 m stepped placement layer.....	28
Figure 3.8: 3D Extrapolated slope illustration, Courtesy of Slide 3 .....	30
Figure 3.9: 3D composite slope illustration .....	30
Figure 4.1: 2D Slope cross-section with 5m stepped placement layer.....	35
Figure 4.2: 2D Slope cross section with 3.5 m stepped placement layer .....	36
Figure 4.3: 2D Slope cross section with 2.5 m stepped placement layer .....	36
Figure 4.4: 2D Slope cross section with 1.5 m stepped placement layer .....	36
Figure 4.5: Sloped cross section with 5m stepped placement layer .....	37
Figure 4.6: Sloped cross section with 5m stepped placement layer .....	37
Figure 4.7: 2D deterministic FOS comparison.....	38
Figure 4.8: 3D extrapolated deterministic FOS comparison.....	38
Figure 4.9: 3D composite deterministic FOS comparison .....	39
Figure 4.10: Auto Refine Search versus Cuckoo search Method results using Slide 2 .....	40
Figure 4.11: 2D, 3D Extrapolated and 3D Composite factor of safety frequency graph with tail spike .....	41
Figure 4.12: 2D, 3D Extrapolated and 3D Composite factor of safety frequency graph with controlled spikes .....	42
Figure 4.13: 2D slopes versus 3D extrapolated slopes comparison .....	43
Figure 4.14: Unsafe analysis set for ideal case for 3D analysis .....	44
Figure 4.15: Unsafe analysis set for worst-case for 3D analysis.....	45

Figure 4.16: Unsafe analysis for ideal case for 2D analysis .....	47
Figure 4.17: Unsafe analysis for worst-case for 2D analysis .....	47
Figure 4.18: $F_{EXT}$ and $F_{COMP}$ difference vs coefficient of variation .....	49
Figure 4.19: $F_{2D}$ and $F_{COMP}$ difference vs coefficient of variation graph.....	50
Figure 4.20:Low coefficient of variation for 5m internal layered slope .....	52
Figure 4.21: High coefficient of variation for 5m internal layered slope.....	52
Figure 4.22: Low coefficient of variation for 3.5m internal layered slope .....	52
Figure 4.23: High coefficient of variation for 3.5m internal layered slope.....	52
Figure 4.24: Low coefficient of variation for 2.5m internal layered slope .....	52
Figure 4.25: High coefficient of variation for 2.5m internal layered slope.....	52
Figure 4.26: Low coefficient of variation for 1.5m internal layered slope .....	52
Figure 4.27: High low coefficient of variation for 1.5m internal layered slope.....	52
Figure A. 1: RocScience recommended material statistics (Slide 2 & Slide 3).....	63
Figure A. 2: 2D probabilistic probability of failure comparison graph.....	63
Figure A. 3: 3D extrapolated probabilistic probability of failure comparison graph.....	64
Figure A. 4: 3D composite probabilistic probability of failure comparison graph .....	64
Figure B. 1: Sample Record book illustration for Morgenstern and Price.....	66
Figure B. 2: Record book illustration of Results from Spencer Method.....	66
Figure B. 3: Typical abnormal section .....	67

## Abbreviations and symbols

2D	2 Dimensional	This is geometric plane which considers 2 axis to determine the slopes' coordinate values
3D	3 Dimensional	This is geometric plane which considers 3 axis to determine the slopes' coordinate values
FOS	Factor of safety	Ratio of slope stabilizing forces and potential destabilizing forces
$F_{EXT}$	Factor of safety of 3D extrapolated (extruded) slope section	The factor of safety for a 3 D slope section originating from the extrapolation of a 2D cross sectional slope model. It is analysed using 3-Dimensional slope stability method
$F_{COMP}$	Factor of safety of 3d composite slope section	The factor of safety for a 3 D slope section originating from 3 different 2D extrapolated sections. It is analysed using 3-Dimensional slope stability methods
PF	Probability of Failure	The ratio of failing slopes to the total number of slope models analysed

## List of published papers

The following paper is based on work contained in this report:

MacRobert, CJ, de Koker, N, Mutede, T. 2021. In Proc. “Can 2D cross sections be safely extrapolated?” *Rocscience 2021 international conference*: Rocscience

## Chapter 1: Introduction

### 1.1 Background and Justification

Earth slopes may be natural or man-made. Natural slopes occur due to geomorphological processes such as erosion and deposition (Atkinson, 2007). Man-made slopes are constructed as a result of engineering activities among which include road and dam embankments; excavations and open cast mines; buildings and dam foundations slopes. In South Africa, slope stability problems include tailings dams, landfills, and laterally supported slopes using retaining walls, road excavation, and embankment dams. These earth slopes require good design and continuous monitoring in order to ensure stability and human safety. This design and monitoring requires safe methods to model slopes and analyse them for stability.

Limit Equilibrium Methods (LEM) and Finite Element Methods (FEM) are common slope stability analysis approaches (Atkinson, 2007). These approaches determine a factor of safety (FOS) in order to assess the stability of a slope (Chakraborty & Goswami, 2018). The ratio of resisting forces to destabilizing forces experienced by a slope is known as the FOS. These approaches can be carried out using either two-dimensional (2D) or three-dimensional (3D) models of the slope in order to determine the FOS (Whitlow, 1995).

Historically, 2D methods have been used to analyse slopes and determine factors of safety due to the lack of 3D computational techniques. 2D methods investigate slope stability by analysing a two-dimensional cross-sectional of a slope. 3D methods investigate the stability of slopes by analysing a three-dimensional model of the slope. The main difference between these two methods lies in the assumptions made to solve force equilibrium and moment equilibrium. 3D methods require more assumptions due to the additional plane under consideration.

It is common practice to generalize soil properties when analysing slope models. The effects of soil variability should, however, be taken into consideration. Variability emanates from the soil within the slope having different properties (e.g. unit weights, cohesion, or friction angles) at different points. During slope stability analysis, even with the consideration of soil variability, it is still unclear as to which method is more effective (i.e. 2D or 3D).

As technological advances and software analysis capabilities have increased, so too has the reliance on the use of 3D models to analyse slopes (Stark & Ruffing, 2017). Often in practice 2D cross-sections are extruded in order to generate 3D models. This simplification, however, raises

uncertainties during analysis since the weaker regions along the slope might be overlooked. Ultimately it might be safer to rely on 2D models.

At present, there is little information on which slope analysis procedure is the safest. Currently, experience and judgment are the main tools relied upon when making the final call on the most critical results. Therefore, research is necessary in order to determine whether the use of extrapolated cross-sections to generate 3D slopes is safe when the influence of spatial variability is taken into account.

This project has relevance in the geotechnical engineering industry, especially in the design of tailings dams. When analysing low-risk slopes using 2D methods, specified safety factors are recommended (Stark & Ruffing, 2017). These safety factors are used in order to account for risks and uncertainties that may exist within the slope's geometry and its internal soil properties. When 3D methods are used to design and analyse slopes, practicing engineers might still rely on the same recommended safety factors for 2D methods despite there being more uncertainties. This poses a risk as there is little knowledge on whether this is safe or not. If tailings facilities are designed with the use of the more modern 3D approach, it is difficult to know whether the design would be robust enough to prevent events such as dam failure and breaching from tailings material. This is further complicated by the heterogeneous nature of the slope's soil. It is for these reasons that this research study is of interest.

## 1.2 Objectives and aims

Extrapolated cross sections may conceal the underlying spatial variability which may lead to lower localised 3D factors of safety. Consequently, it may be safer to rely on 2D factors of safety compared to 3D factors of safety in design of slopes. The objective of this study was therefore to investigate the risk associated with extrapolating 2D cross sections to carry out 3D slope stability analyses with specific reference to tailings dams.

The specific aims of this study were as follows:

- Generate multiple 2D and 3D slope scenarios, varying within distinct soil boundaries.
- Carry out 2D and 3D slope stability analysis, using commercially available software.
- Compare the resulting 2D and the 3D factors of safety in order to understand the reliability associated with the two approaches.

### **1.3 Limitations and challenges**

The scope of the study was limited to:

- Considering one single external geometry with multiple internal geometries due to each slope stability simulation being set up manually. The time required for this manual set-up made it unfeasible to analyse multiple external geometries
- Geometry and internal boundary characteristics of upstream tailings dams.
- Utilising the Rocscience Slide 2 and Slide 3 computer programs.

### **1.4 Report Structure**

This thesis consists of 5 Chapters:

- Chapter 1 introduces the study, outlines the objectives and list limitations of the research.
- Chapter 2 gives a review of relevant slope stability literature. Concepts and theories for modelling slope stability are discussed.
- Chapter 3 presents an outline of the methodology which was followed in the research.
- Chapter 4 presents the results obtained from the slope stability analysis simulations. This chapter also gives the analysis and discussion of results obtained, focusing on the comparison between 2D, 3D extrapolated and 3D composite factors of safety.
- Chapter 5 offers various conclusion and recommendations for carrying out safe 3D slope stability analysis for upstream constructed tailings dams.

## Chapter 2: Literature review

### 2.1 General

This chapter presents concepts, theory and literature on slope stability analysis. Although the project is about slope stability analysis, it has specific reference to tailing dams. Consideration is therefore given to the design, construction and operation of tailings dams.

### 2.2 Tailings dams

Tailings are by-products generated from the separation of valuable material from rock or soil during mining activities (MAC, 2019). Tailings normally consist of sand, silt and clay sized particles. Due to tailings being formed through mining activities, they may contain harmful substances which are toxic to the environment. For this reason, good storage methods have to be implemented in order to safely contain the material.

There are a number of tailings containment methods that are used including open pits, ponds and tailings dams (ANCOLD, 2012). Tailings dams are man-made embankments which are used to store mining by-products in a safe and confined manner. There are two main types of tailings retaining embankments: cross valley impoundments and off valley impoundments.

Cross valley embankments utilise surrounding topography to store tailings. The layout is similar to that of a water dam with embankments being placed across a valley. Generally, they have a small earthwork volume per unit of storage (ANCOLD, 2012). Off-valley impoundments rely on longer embankment lengths, giving them a larger earth work volume per unit storage. Off-valley impoundments include side hill impoundments which rely on three-sided embankments and fully contained ring dykes with embankments on all sides (ANCOLD, 2012).

In general, embankments for tailings have two main functions. These functions are the containment of water and solids. Embankments that retain water and solids are built similarly to water storage dams with similar features such as low permeability clay zones, filters, liners and drainage features in order to limit seepage. Embankments that are built for the retention of solids, often do not incorporate as many engineered features, but still require filter or drainage zones in order to promote safe passage of seepage (ANCOLD, 2012).

It is common practice to construct tailings dams in stages as it is often uneconomical to build tailings dams to full height at the start. For this reason, the use of the self-staking methods is useful in tailings dams. Construction begins with a starter embankment, providing storage for

about three years after which the wall is raised by self-stacking construction. This is advantageous as it allows tailings to be included as part of the construction material of the tailings dam. Along with the starter embankment, features to control seepage, such as liners, under drainage and foundation cut offs are usually constructed simultaneously (ANCOLD, 2012).

### **2.2.1 Methods of construction**

The most common tailing dam construction method is self-stacking. Self-stacked tailings dams make use of dried tailings material for building. The self-stacking method is particularly advantageous due to low construction costs due to readily available construction material (ANCOLD, 2012). However, this method may not be suitable for rainy regions as insufficient drying may take place to form competent construction material.

Three key methods of the self-stacking include upstream, downstream, and centreline construction.

#### **2.2.1.1 Upstream construction**

In this method, a starter embankment is first constructed. Tailings are placed behind the starter embankment as is shown in Figure 2.1. A dike, consisting of coarse material, is then developed with already placed tailings forming the foundation for the next level of the embankment. As more material is added, the crest of the embankment rises upstream whilst being supported by underlying foundation from the previously settled tailings material. This is carried on until the design height of the embankment is reached. The stability of this method is dependent on the strength of the tailing material themselves (Vick, 1990).

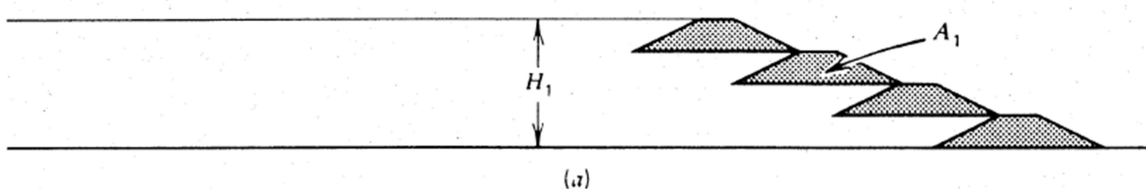


Figure 2.1: Upstream construction (Vick, 1990)

#### **2.2.1.2 Downstream construction**

Similar to upstream construction, a starter dam is initially constructed. A low permeability zone is generally included in the wall. Consequently, internal drains are often incorporated in the construction process. Tailings are collected and deposited on the downstream end of the starter dam, with each new crest being higher than the previous crest height. This in turn raises the embankment and forms a new higher crest on the downstream as shown in Figure 2.2. In

general, this form of construction is considered more stable than upstream construction however, it requires more material (Vick, 1990).

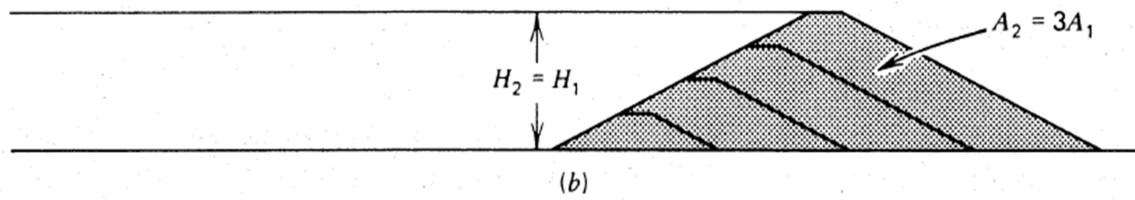


Figure 2.2: Downstream construction (Vick, 1990)

### 2.2.1.3 Centreline construction

This method has similarities to both the upstream and downstream construction methods. A starter dam is first developed, with wall raising taking place on both the upstream and downstream sides. The embankment rises vertically on a centreline without favouring the downstream or upstream sides (Vick, 1990). Figure 2.3 shows the cross section typically developed with this method.

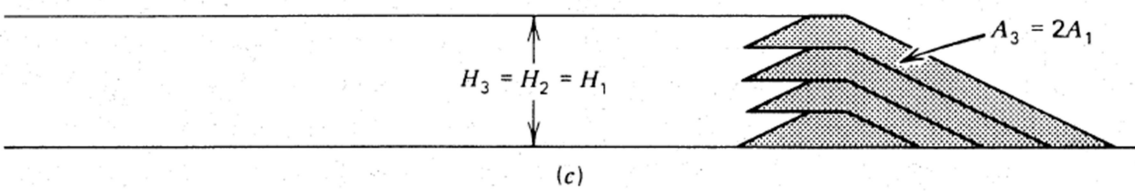


Figure 2.3: Centreline construction (Vick, 1990)

## 2.2.2 Tailings dam design

The design of tailings dams is dependent on a number of factors, amongst which include the characteristics of the tailings, the material used to construct the dam, and the physical characteristics of the region (Vick, 1990). The location of the tailings dam's phreatic surface is a major consideration in the design process. Design of the material arrangement has to favour a phreatic surface that remains as low as possible from the embankment face. Control of the phreatic surface dictates the type of material required for construction and the configuration in internal zones (Vick, 1990). The material configurations become the sources of heterogeneity within tailings dams.

## 2.2.3 Tailings dam analysis methods

Limit Equilibrium procedures are a common method of analysing tailing dam embankment stability. The Finite Element Method is another method that can be used where it is crucial to

determine the deformation to be experienced by tailings dam as well as the pore water pressure. This is of significance as it relates to the upstream construction where materials are exposed to strain leading to their softening over time. It can also be used in situations when liquefaction is a possibility (ANCOLD, 2012).

The loading conditions are a crucial facet that requires consideration before conducting an analysis. Loading conditions are a representation of the physical conditions experienced by the tailings dam that needs to be analysed. This analysis is carried out with specific types of material strengths which mimic the conditions being experienced on the ground (ANCOLD, 2012). The contractive nature of the tailing dam material also needs to be considered.

The following conditions should be considered for the analyses of tailings dams:

#### **2.2.3.1 Drained Conditions**

Drained situations are normally known as long-term conditions or steady-state conditions (Duncan et al. 2014). In this condition, the excess pore water pressures caused by the initial loading of the structure have dissipated. Shear-induced pore pressures also dissipate due to the presence of a slow shearing rate during failure. The materials in this condition are represented by effective stresses and drained shear strength. Situations in which drained loading conditions can be experienced include the long-term static stability at the ultimate design height and the long-term post-closure stability of a tailings dam.

#### **2.2.3.2 Undrained Conditions**

Undrained conditions are the conditions experienced in the short term during which loading of the soil occurs quickly such that insufficient time is available for drainage of induced excess pore pressures (Duncan et al. 2014). Although some drainage does occur, it is often difficult to determine the location along the shear surface where it occurred. The best way to tackle the challenge posed by this uncertainty is to use an undrained strength envelope to check the stability of the tailings dam. These conditions can be experienced in a soft clay foundation or in saturated contractive tailings. Another phenomenon that should be monitored is that of static liquefaction. This is where large pore pressures develop and lead to zero effective stresses being developed due to a brittle stress-strain response. This must be considered while evaluating the undrained loading conditions.

## 2.3 Tailings dams site investigations

In order to correctly model tailings dam embankments and perform slope stability analyses, site investigations have to be carried out to determine embankment properties. Investigation methods include in situ tests and laboratory tests (Wei, 2016).

### 2.3.1 In situ tests

The use of rotary machines to drill boreholes in situ is a common method used to conduct subsurface exploration of tailings dams (Wei, 2016). From the boreholes, core samples are collected for further study in the laboratory for further testing. Alongside drilling, in situ testing methods can be carried-out to obtain further information on the subsurface conditions in tailings dams. The Cone Penetration Test (CPT), and Standard Penetration Test (SPT) are two common tests that are conducted.

Cone Penetration Tests (CPT) are one of the most important soil investigating techniques for tailings dams. A cone penetration device is pushed into the ground at a predetermined rate. While being inserted into the ground, the soil's response is measured. This can be done for depths of up to 100 meters. Readings from the CPT are then used to determine tailings dam's soil properties via correlations (Robertson and Cabal 2012). Standard Penetration Testing (SPT), involves applying standardised blows onto a sample tube in order to penetrate into the ground. The number of blows required to penetrate a standard depth are recorded. The information is then used together with geotechnical correlations to determine soil properties (Atkinson, 2007).

The locations where in situ tests are conducted are normally selected in order to determine a typical cross-section through the embankment. Multiple cross-sections may be determined based on the size of the tailings dam. Figure 2.4 shows an illustration of a site investigation carried out on a tailings dam. Sampling lines were chosen on the tailings dam's downstream face. For each line, boreholes and penetration test were done to determine the tailing dam's profile and conditions (Wei, 2016).

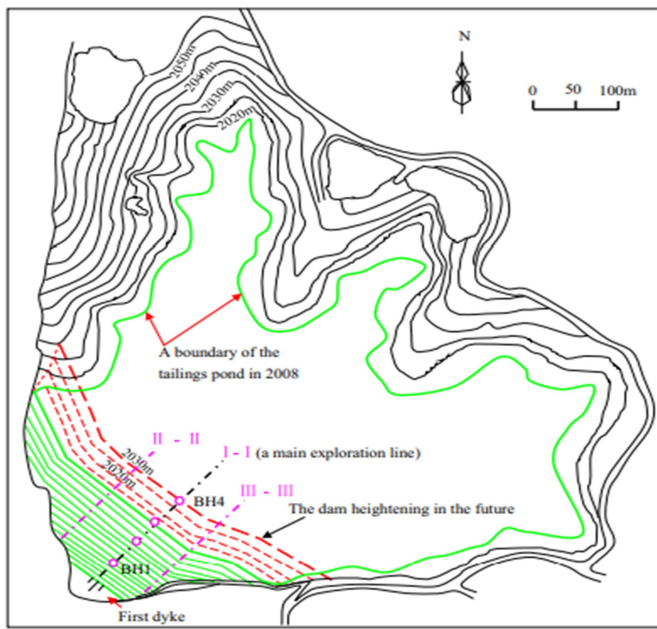


Figure 2.4: Schematic of a typical tailings dam site investigation (Wei et al 2016)

### 2.3.2 Laboratory tests

Collected soil samples from borehole drillings and test pits are tested in the laboratory in order to determine soil properties of tailings dams. Common laboratory tests include particle size analyses to classify the different types of soil that makes up the soil; specific gravity tests which helps in the determination of additional soil properties such as void ratio and degree of saturation; and Atterberg limit tests to establish the shrinkage, plastic and liquid limits for fine grained soil material (Budhu, 2011). In addition, shear tests are also carried out to determine shear strength. Shear tests are commonly conducted using two methods: Direct shear strength and Triaxial shear tests (Bhanbhro, 2017).

The Direct shear test is conducted using a shear box test. An undisturbed soil sample is placed into the shear box consisting of a top and bottom half. A confining stress is applied vertically to the specimen, while a horizontal shearing force is introduced in-between the top and bottom half of the shear box. This is continued until the sample fails or a specific strain is reached. Through the constant measurement of the load and stress experienced, the stress strain curve of the soil sample can be determined. The shear strength characteristics of the soil, i.e. the soil cohesion and friction angle, are then calculated (Bhanbhro, 2017).

In the Triaxial shear test, a soil sample is placed into a flexible and impermeable membrane in a triaxial cell. The cell is placed onto the loading frame of a triaxial shear machine where it is subjected to a vertical load. A fluid is also introduced into the cell in order to apply horizontal

pressure to the soil sample while inside the impermeable membrane. Confinement pressures are set to meet in-situ conditions. The soil sample is then tested during a consolidation phase and a shearing a shearing phase. From the results of the test the shear strength of the soil can be determined (Duncan et al. 2014).

## 2.4 Slope stability analysis

The limit equilibrium and finite element methods can be used for slope stability analysis. While this study focuses on the limit equilibrium method a brief discussion of the finite element method is also given. Two-dimensional methods have been extensively used to analyse slopes and determine factors of safety (Chaudhary et al. 2016). However, due to new developments and computational advances 3D methods are becoming popular. The following sections outline key aspects in this development.

### 2.4.1 Two-dimensional limit equilibrium approaches

For this approach, slip surfaces are assumed to have a circular or non-circular nature. A 2D model of the sliding body of soil is considered. The 2D cross-section is divided into a number of vertical slices (Chakraborty & Goswami, 2018). For each slice, the stresses experienced by the slice are determined by considering each slice's equilibrium conditions. In doing this, the stability of the slope is determined by calculating the factor of safety for the slip surface. Figure 2.5 shows a slope's cross-section along with a circular failure plane which has been divided into slices.

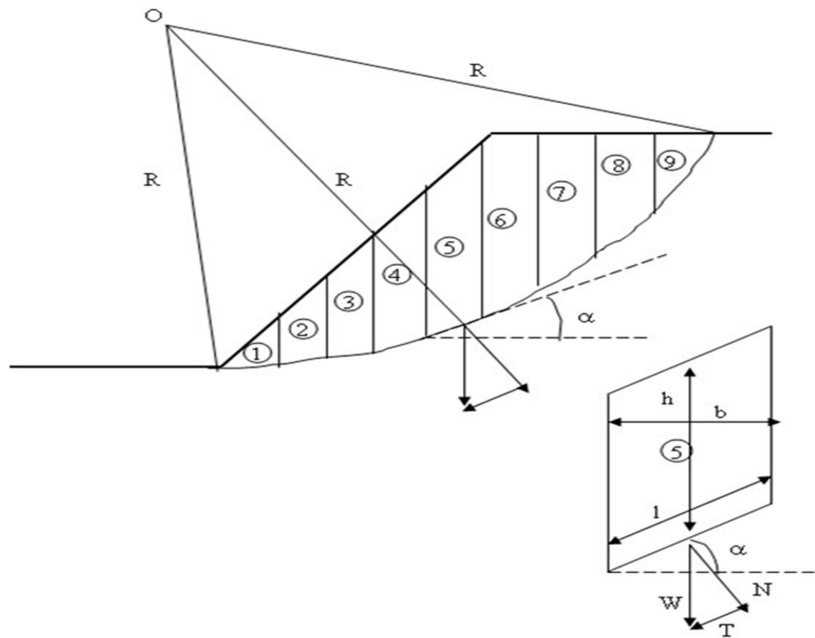


Figure 2.5: Slope cross section, sliding mass, slices and variables associated with each slice (Ranjan & Rao, 2000)

- $R$  = Radius
- $\alpha$  = angle between the tangent of the centre of the base of each slice and the horizontal
- $h$  = Mean slice height
- $b$  = Slice width
- $l$  = Length of slice base
- $W$  = Weight of Slice
- $N$  = Total Normal force at the base
- $T$  = Shear force on the base of the slice

Due to the equations for determining the slope's stability being indeterminate, various assumptions are made in order to make the problem determinate (Chakraborty & Goswami, 2018). These assumptions include ignoring inter-slice forces, regarding or neglecting moment equilibrium experienced by slices. With each assumption, a different technique of solving the safety factor is established. Some methods only meet some equilibrium criteria (i.e. either force equilibrium or moment equilibrium), while others meet all equilibrium criteria and thus are more accurate (Duncan et al. 2014). Table 2.1 and Table 2.2 summarises the 2D limit equilibrium methods.

**Table 2.1: Limit Equilibrium Methods (LEM) Summary Table (reproduced from Duncan et al. 2014)**

<b>Procedure</b>	<b>Equilibrium Condition Satisfied</b>	<b>Shape of slip surface</b>	<b>Assumptions</b>	<b>Unknowns Solved for</b>
Simplified Bishop Method	Vertical equilibrium and overall moment equilibrium	Circular	All interslice shear forces are zero due to the forces on the sides of slices being assumed horizontal	<ul style="list-style-type: none"> <li>• <math>I</math> Factor of safety,</li> <li>• <math>n</math> Normal forces acting at the base of slices (N)</li> <li>• <math>n + 1</math> Total unknowns</li> </ul>
Logarithmic Spiral Method	Moment Equilibrium about centre of spiral	Log spiral	The slip surface is a logarithmic spiral.	<ul style="list-style-type: none"> <li>• <math>I</math> Factor of safety = 1</li> <li>• Total unknown</li> </ul>
Janbu's Simplified Method	Force equilibrium (vertical and horizontal)	Any shape	The side forces are horizontal.	<ul style="list-style-type: none"> <li>• <math>I</math> Factor of safety,</li> <li>• <math>n</math> Normal force acting at the base of slices (N)</li> <li>• <math>n-1</math> Resultant interslice forces (Z)</li> <li>• <math>2n</math> Total unknowns</li> </ul>
Spencer's Method	All conditions of equilibrium	Any shape	<p>Interslice forces are parallel (i.e., all lie at the same angle).</p> <p>The normal force (N) acts at the centre of the base of the slice.</p>	<ul style="list-style-type: none"> <li>• <math>I</math> Factor of safety</li> <li>• <math>I</math> Interslice force inclination (<math>\Theta</math>)</li> <li>• <math>n</math> Normal force on the base of slices (N)</li> <li>• <math>n-1</math> Resultant interslice forces (Z)</li> <li>• <math>n-1</math> Location of side forces (line of thrust)</li> <li>• <math>3n</math> Total unknowns</li> </ul>
Morgenstern and Price's Method	All conditions of equilibrium	Any shape	<p>Interslice shear force is related to interslice normal force by: <math>X = \lambda f</math></p> <p>(x) E</p> <p>The normal force acts at the centre of the base of the slice.</p>	<ul style="list-style-type: none"> <li>• <math>I</math> Factor of safety</li> <li>• <math>I</math> interslice force inclination “scaling factor” <math>\lambda</math></li> <li>• <math>n</math> Normal force acting at the bottom of slices (N)</li> <li>• <math>n-1</math> Horizontal interslice forces (E)</li> <li>• <math>n-1</math> Location of interslice forces (line of thrust)</li> <li>• <math>3n</math> Total unknowns</li> </ul>

**Table 2.2: 2D Limit Equilibrium Methods Applications Summary Table (reproduced from Duncan et al. 2014)**

Method	Use
Simplified Bishop Method	<ul style="list-style-type: none"> <li>This method is appropriate for non-homogenous slopes and applicable for cohesion and friction soils where circular slip surfaces are utilised.</li> <li>In comparison to the Ordinary Method of Slices, this method delivers more accurate findings, especially for slope studies with high pore water pressures.</li> <li>Calculations can be easily executed using hand calculation or spread sheet.</li> </ul>
Logarithmic Spiral Method	<ul style="list-style-type: none"> <li>This method is suitable for homogeneous slopes.</li> <li>The method is also particularly useful for developing slope stability charts and is used certain software for reinforced slope design.</li> </ul>
Janbu's Simplified Method	<ul style="list-style-type: none"> <li>Suitable for any shape of slip surface.</li> <li>Suitable for the rigorous analysis.</li> </ul>
Spencer's Method	<ul style="list-style-type: none"> <li>This is a very accurate procedure which can be applied to a diverse group of slope geometries and soil profiles. This method is one of the simplest complete equilibrium procedures for determining the factor of safety.</li> </ul>
Morgenstern and Price's Method	<ul style="list-style-type: none"> <li>A accurate method that works with a variety of slope geometries and soil profiles.</li> <li>A well established and complete equilibrium process that is very rigorous.</li> </ul>

#### 2.4.2 2D cross section development approach

Following the acquisition of site investigation information, a better understanding of the cross-sectional slope properties is established. The slopes' material property information together with the soil layering and ground water information is utilized in the modelling procedure (Chaudhary et al 2016). In addition, topography information, determined from surveying or satellite information, is utilized. With this information, a 2D cross-section of the slope can be generated in order to perform analysis.

### **2.4.3 3D Slope stability analysis**

Three-dimensional slope models are an extension of 2D models. This approach aims at developing a means of analysing slopes with intricate geometries which normal 2D methods cannot analyse thoroughly. This is suitable for slopes whose topography varies dramatically in the longitudinal direction (Kalatehjari & Ali, 2013). This is due to 3D analyses accounting for the third dimension. The method is useful when the material properties of the slope being analysed has a heterogeneous nature. This can occur when a slope has multiple soil layers with varying thicknesses in the longitudinal direction of the slope.

There are a number of software available on the market worldwide that analyse the stability of slopes using 2D and 3D techniques. The level of accuracy of their analysis is often dependent on the level at which the generated model being analysed matches that of real life. The software is also dependent on the ability of the user to generate a realistic model. In addition, the method of analysis of the model also influences results based on the software's programmed assumptions and analysis techniques. For this reason, there is not one widely recognised slope stability program for 3-Dimensional slope analyses (Stark & Ruffing, 2017).

### **2.4.4 3D cross section development approach**

Similar to 2D approaches, soil profile information from the site investigation stage is used together with topographical data to develop 3D slope models (Chaudhary et al 2016). Often, a 2D cross-section of the slope is generated before it is extruded(extrapolated) for a predetermined longitudinal distance. In doing so, a 3-dimensional model is in turn generated to which material properties can be added to complete the modelling process (Kalatehjari & Ali, 2013).

### **2.4.5 3D limit equilibrium slope stability methods**

A number of 3D limit equilibrium methods are available and are largely an extension of familiar 2D methods of slices with slices considered as 3D columns. Ultimately, the conditions of limit equilibrium for each column has to be met in order for the slope to be deemed stable. Most assumptions made for 3D approaches come from 2D analysis, however additional assumptions are required as there are extra unknowns (Stark & Ruffing, 2017). Table 2.3 gives a summary of a few 3D limit equilibrium methods.

**Table 2.3: 3D Limit Equilibrium Methods (LEM) Summary Table (Aktahr, 2011)**

Procedure	Theoretical basis for 3D assumption	Equilibrium Condition Satisfied	3D shear surface shape	Assumptions
Hungr (1987) Hungr et al (1989)	Bishop's simplified method	Vertical force and overall moment equilibrium	Symmetrical	<ul style="list-style-type: none"> <li>The side forces are horizontal (i.e. all interslice shear forces are zero.)</li> </ul>
Huang, Tsai and Chen (2002)	Janbu's generalized procedure	Horizontal and vertical force and moment equilibrium	asymmetrical	<ul style="list-style-type: none"> <li>The side forces are horizontal (i.e. all interslice shear forces are zero.)</li> </ul>
Agnanotsi (1969)	Morgenstern and Price method	Horizontal force, vertical force and moment equilibrium	Unspecified	<ul style="list-style-type: none"> <li>Limit equilibrium is satisfied on each side of the sliding mass</li> </ul>
Lam and Frendlund (1993)	Morgenstern and Price method	Horizontal force, vertical force and moment equilibrium	Ellipsoidal	<ul style="list-style-type: none"> <li>Similarly, to Morgenstern and Price method, Interslice shear force is related to interslice normal force by: <math>X = \lambda f(x)E</math></li> <li>5 interslice force functions are used</li> </ul>
Chen & Chameau (1983)	Spencer's method	Horizontal force, vertical force and moment equilibrium	Ellipsoidal	<ul style="list-style-type: none"> <li>The interslice forces have the same angle throughout the mass. As a result, shear forces have the same angle as the column base</li> </ul>

#### 2.4.6 Comparison of 2D and 3D slope stability analysis

Studies comparing 2D and 3D slope stability analysis have focused on homogenous soil conditions. Researches have found that in general, 3D factors of safety are generally higher than those from 2D approaches (Albataineh, 2006). Table 2.4 gives a summary comparison of the previously mentioned 3D methods against 2D slope stability methods.

**Table 2.4: 2D vs 3D slope stability analysis comparisons**

<b>3D Slope stability analysis procedure</b>	<b>Equivalent stability procedure</b>	<b>2D slope analysis</b>	<b>2D versus 3D slope stability analysis results</b>
Hungr (1987) Hungr et al (1989)	Bishop's simplified method		3D factor of safety values were higher than corresponding 2D factor of safety values. However, conservative 3D results were obtained due to neglecting internal shear forces (Kalatehjari & Ali, 2013).
Huang, Tsai and Chen (2002)	Janbu's generalized procedure		3D results yield similar results to Lam and Frendlund's slope stability analysis results. The 3D factor of results were greater than the 2D factor of safety results (Huang, 2002).
Agnanotsi (1969)	Morgenstern and Price method		3D factor of safety values experienced a 50% increase from the original 2D factor of safety values obtained (Kalatehjari & Ali, 2013).
Lam and Frendlund (1993)	Morgenstern and Price method		It was determined that the 3D method was not affected by intercolumn force function. The 3D factor of safety values were found to be higher than the 2D factor of safety (Kalatehjari & Ali, 2013).
Chen & Chameu (1983)	Spencer's method		3D slope stability analysis results were found to be 10% lower than 2D results when low cohesion and high cohesion soils were analysed. However, 3D results were found to be higher than 2D results when pore water pressure was present (Kalatehjari & Ali, 2013).

#### 2.4.7 Acceptable factors of safety

The interpretation of factors of safety is subjective due to model and material uncertainties. There are however, recommended factors of safety values based on precedent documented in tailings dam guidelines. Examples include guidelines produced by the Australian National Committee (ANCOLD), International Commission of Large Dams (ICOLD) and Anglo American, which are summarised in Table 2.5.

**Table 2.5: Recommended factors of safety based on (ANCOLD, 2012) and (Anglo-American, 2019) and (ICOLD, 2020)**

<b>Recommended Minimum for Tailings Dams (ANCOLD and ICOLD)</b>	<b>Recommended Minimum for Tailings Dams (Anglo-American)</b>	<b>Shear Strength to be Used for Evaluation</b>
Long term, drained	1.5	Effective strength
Short term, undrained (potential loss of containment) & (no potential of containment)	1.3-1.5	Consolidated undrained strength
Post seismic	1-1.3	Post seismic shear strength

#### 2.4.8 Probabilistic analysis of slopes

An additional way to assess safety is by utilising probabilistic approaches. The Monte Carlo method is one such technique that can be used. This technique is used for estimating the uncertainty in a slope stability analysis (Malkawi et al. 2003) by randomly generating soil parameters and considering multiple slip surfaces. Probabilistic approaches result in a distribution of factors of safety, from which a reliability index can be calculated (Shehata et al. 2018). This increases the amount of information being considered in the decision. Furthermore, research has found that probabilistic approaches, generally improve the chances of finding critical surfaces. This is because more rigorous analyses results are obtained due to uncertainties, caused by the variable nature of soils, being considered (Shehata et al. 2018).

## 2.5 Spatial variability

Properties within tailings embankments vary from location to location. This heterogeneity in properties, is termed spatial variability (Varkey et al. 2017). In natural soils, spatial variability is due to geological, chemical and environmental processes varying from location to location (Varkey et al. 2017). In tailings embankments spatial variability can also be caused by these natural processes, but depositional and construction processes introduce greater heterogeneity.

When tailings dams are constructed, hydraulic filling techniques are normally used (Blight, 1983). This consists of conveying tailings material (slurry) through pipelines and depositing the material to build up the tailings dam wall. During the deposition period, coarser materials settle at a faster rate than fine materials. This results in a gradation of particles as one moves down a tailings beach due to hydraulic sorting of deposited material (Blight, 1983).

Different cross-sections can be formed during the material deposition phases. If the solid content and coarseness within the slurry increases, this can result in steeper beaches profiles being built (Blight, 1985). Furthermore, due to hydraulic sorting during deposition, fine material (e.g. clay and silt) is usually located in the centre of the dam and coarser material (e.g. sand) close to the embankment. This results in the outer section often being drier and more competent within inner sections remaining wet and weak (MacRobert & Blight, 2013). Figure 2.6 shows a typical illustration of the tailings cross section that is developed from the tailings material deposition phase of an upstream constructed tailings dam.

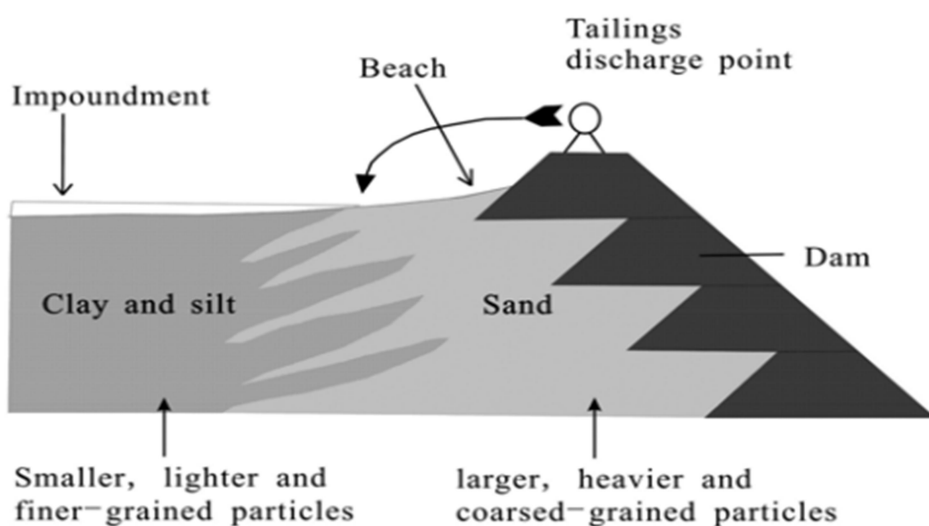


Figure 2.6: Tailings Dam cross section with typical beach illustration (Pan et al. 2017)

The sorting of material particles results in varying properties within the tailings section. This heterogeneity in properties results in the spatial variable nature of a tailings dam wall. Both limit equilibrium and finite element methods have been used to study spatially variable slopes.

### **2.5.1 2D studies on spatial variability**

Fenton and Vanmarcke (1990) proposed that spatial variability could be considered using a random field. In this approach a field is divided into a grid with each cell assigned randomly generated soil parameters. Cell values within close proximity are given similar soil parameters based on the spatial correlation length. Soil parameters along a slip surface are then retrieved based on the relative location to the field. Limit equilibrium methods are then used to establish the FOS. The probability of failure can then also be calculated by running several simulations (Shehata et al. 2019). Random field parameters can also be mapped to points on a finite element mesh (Varkey et al. 2017) and FOS calculated using the shear strength reduction approach (Varkey et al. 2017). The FOS is calculated by dividing the resisting shear strength by the resisting shear strength along the failure plane (Chatterjee et al 2012). Again, a distribution of FOS can be determined by carrying out a number of runs (Varkey et al. 2017).

Su and Liao (1999) used 2D slope stability analysis to investigate the effects of strength anisotropy on an undrained slope. The strength anisotropy was due to varying shear strength resulting from inherent anisotropy of clay (Sui and Liao, 1999). Two undrained shear strength scenarios were analysed. The first scenario had a relationship between the undrained shear strength and the inclination of the failure plane, while the second scenario had no relationship. The isotropic factor of safety ( $F_{SI}$ ) was initially determined using undrained shear strength ( $S_{UI}$ ). The anisotropic factor of safety was then determined using a correlation ratio ( $F_{SA} / F_{SI}$ ).

Three elements were found to have an impact on the correlation ratio (i.e.  $F_{SA} / F_{SI}$ ). The first was the strength anisotropy ratio ( $A_R$ ). The smaller the correlation ratio was, the more significant the influence of anisotropic strength. The second factor that influenced the ratio was the undrained strength. It was found that the greater the values of undrained strength ( $S_{UI}$ ) used, the more likely the value of isotropic factor of safety ( $F_{SI}$ ) would be overestimated. This in turn would have an influence on the accuracy of the anisotropic factor of safety ( $F_{SA}$ ). Lastly, the location of the slip surface was found to have an influence on the correlation ratio. The effects of strength anisotropy were found to increase if large sections of the slopes section were under lateral compression (Sui and Liao, 1999). This can be witnessed on deep base slope failures. Ultimately it was concluded that the level of anisotropy experienced by the soil had an influence

on whether the anisotropic factor of safety would correspond to the isotropic factor of safety. This highlighted the intricacies encountered with soil variability and how overestimations of slope's true stability have to be considered when performing analyses.

Hwang et al. (2002) investigated the effects of strength anisotropy in 2D excavated clay slopes. The potential slip surface was modelled through sequential excavation and analysis of a ground surface until it reached a critical stress state (Hwang 2002). Finite element modelling was used through a program named CRISP. The finite element program was used to generate a mobilized friction angle and stress ratio. These were used in the slope analysis to determine whether extension regions within the slope experienced anisotropic conditions. Results showed that the observed slope failure did indeed experience anisotropic behaviour, and it occurred regardless of what stress state, strength condition, or slope angle was experienced (Hwang et al. 2002). The anisotropic behaviour was a result of progressive failure being experienced by the slope. It was concluded that the inclusion of strength anisotropy would result in lower, more conservative safety factors being calculated compared to those derived using isotropic strength (Hwang et al. 2002).

Le et al. (2014) investigated the stability and failure of unsaturated heterogeneous slopes. The effects of having heterogeneous void ratio in a slope with unsaturated conditions exposed to rainfall were investigated. With the use of a Monte Carlo framework, the sliding masses and factors of safety were determined using a 2D model analysed using a random finite element method. Slope simulation was done before and after rainfall infiltration. The factor of safety and the size of failure surface were then determined four times for each set of infiltration period. By increasing the void ratio and the correlation over a longer distance the spatial variability of the soil was increased. When this was achieved it was found that the probability of slope failure increased with the increase of variability in the soil (Le et al. 2014). This was deduced from an increase in the range of varying factor of safety obtained after analyses.

### **2.5.2 3D slope stability studies**

Hicks & Spencer (2009) considered spatial variability in a 3D undrained slope. The soils undrained shear strength, was represented using a normal distribution as well as using point and spatial statistics (Hicks & Spencer, 2009). Random fields of spatial variability were created using the undrained shear strength statistics and a 3D Local Average Subdivision (LAS) algorithm. The horizontal fluctuation was used together with the vertical fluctuation to define the distance over which a slope's property was correlated.

Through finite element analysis of the slope in three dimensions (3D) it was found that after several tests had been done using a Monte Carlo Simulation, three failure modes were found depending on the horizontal fluctuation's relationship with the slope length and height (Hicks & Spencer, 2009). In Mode 1, failure through semi-continuous weaker zones is not possible due to the horizontal and vertical fluctuation scales being too small. Instead, failure occurs in both weak and strong zones, and characteristics are averaged throughout the rupture surface. In Mode 2 failure, discrete failures result due to horizontal fluctuations being large enough for failure to occur through weaker zones. Lastly in Mode 3, failure affects the entire slope length and the failure spreads through weak regions of the slope which gives rise to a larger range of possible failure solutions.

Hicks et al. (2014) further studied the influence of heterogeneous properties on slopes with respect to undrained shear strength. The reliability and failure on a long slope were of key interest. The soil of the slopes was modelled with a spatially variable nature developed using Random Field Theory. The slope was generated in 3 dimensions and was analysed using a finite element package. A Monte Carlo simulation was conducted to determine different failure outcomes through the generation of random slope fields with different undrained shear strengths. The study confirms the 3 Modes of failure mentioned earlier as found by Hicks et al. (2014) in earlier studies. Horizontal fluctuations in the properties of the slope heavily influence the type of 3D failure mode produced. The research also indicated a wide range of different failure surfaces modes and slide geometries experienced for different horizontal fluctuation scenarios which made it difficult to yield any conclusion. This result indicated how challenging it is to study slopes with varying properties in 3D and how difficult it can be to convey variability complexities in 2D analysis.

In a study by Azam et al. (2012) the effects of strength anisotropy on slope stability were studied. The investigation assessed the influence of planes of weakness such as joints and bedding planes. These are generated in natural soils and sedimentary rocks where the ground structure is formed due to deposition and consolidation of soil material. A finite element model was used to perform the slope stability analysis. A Mohr-Coulomb criterion matrix that could incorporate up to 3 planes of weakness was considered by the model. The study looked at the effects of having anisotropic strength in soil material due to the presence of weak planes, and the findings revealed that the material's stability was determined by the presence and configuration of weak planes (Azami et al. 2012). The position of the weak planes determined the form of the

slip surface. This demonstrated the necessity of accurately analysing the 3D profile, since there may be several orientations of weak planes present, resulting in heterogeneous soil characteristics. This also suggested that the extrapolation of 2D sections to create 3D slope models would cause many uncertainties. This is due to unknown variables that arise from the overgeneralising effects caused by the extrapolation of 2D section in 3D slope stability analyses.

The effects of heterogeneous properties on slope stability analysis was studied by Allan et al. (2012). A method called kriging was implemented in order to develop a spatially variable slope. The Kriging created spatially variable conditions by mapping shear strength parameters on random fields of the slope (Allan et al. 2012). Alongside kriging, supplementary spatial interpolation methods were utilized in order to make a comparison to the method. The factor of safety was then calculated using a shear reduction method. It was found that lower factors of safety are obtained from a slope with spatially variable strength parameters than those of homogenous strength value. This effect becomes more apparent the more spatially variable the properties are. All interpolation methods seem to create a smoothing effect which oversimplifies the slopes being analysed. This is due to how heterogeneous properties generate weak regions within the slope mass.

Aghajani et al. (2015) studied the effects of anisotropic shear strength on stability analysis of sandy Slopes. This was done by initially determining the anisotropic friction angle formed as a result of anisotropy in soil. An artificial neural network was created utilizing experimental data from anisotropy tests obtained from the literature to calculate the friction angle. The experimental data comprised of the outcomes of a hollow cylinder torsional shear apparatus's primary stress rotational test (Aghajani et al. 2015). Slope stability analysis was done for anisotropic and isotropic circumstances as a reference through the use of this technique. The results indicated that isotropic conditions have the potential to overestimate factor of safety values as compared to anisotropic conditions by as much as 25%. This however, is more apparent in flatter slopes. It was also found that the geometry of the slope, geometry of the slip surface and shear strength of soil were the most influential factors that influenced anisotropic slope stability. This was found from analysing different slopes of varying heights and lengths under different strength properties for both isotropic and anisotropic conditions.

### 2.5.3 Summary

From the literature review, background information on tailings dams was reviewed in order to gain an understanding on how to best represent and solve the overall research problem. Information on 2D and 3D slope stability analysis methods was also reviewed specifically focusing on the commonly used Limit Equilibrium Methods (LEM). Furthermore, literature on previous slope stability studies on heterogeneous slopes was reviewed in order to gain an understanding of the most influential factors influencing the accuracy of slope stability results.

The literature review has found that, tailings dams are commonly constructed in one of using three methods, namely: Upstream, Downstream and Centreline construction. It is common practice for tailings material to be used during the construction process. During construction, tailings material is deposited at different rates depending on the material's particle sizes. The sorting of material particles results in varying properties within the tailings section. This heterogeneity in properties results in the spatial variable nature of a tailings dam. When analysing slopes, site investigations and laboratory tests are carried out in order to determine the slope's strength. From the information obtained, slope models are developed using 2D or 3D techniques in order to perform slope stability analyses. Previous researchers have found that, 3D Limit Equilibrium Methods typically yield higher FOS values as compared to their 2D Limit Equilibrium Methods.

From the literature, the importance of accounting for spatial variability is highlighted. This has been concluded from historic 2D and 3D slope stability investigations. For both 2D and 3D analyses, it was established that strength anisotropy plays a major role in the slope stability analysis. Previous work also found that it is important to consider overall geometry when performing 3D slope stability analyses. The risk caused by the over generalisation of slope models through extrapolation 2D cross sections, as a result using data from distinct slope regions that have undergone site investigation, still needs to be looked into. This is relevant for tailings dams as they experience varying properties. More research is needed to guide the selection of the most effective analysis method for tailings dams.

## Chapter 3: Methodology

### 3.1 Introduction

This chapter presents the methodology which was developed and implemented in order to achieve the objectives of this research project.

### 3.2 Preliminary modelling

#### 3.2.1 External and internal geometry

A single outer geometry consisting of 30m high slope with a bottom width of 150m and 1:2 outer slope was modelled. Table 3.1 shows the coordinates used to produce the external boundary of the slope.

**Table 3.1: Outer Geometry Coordinates Table**

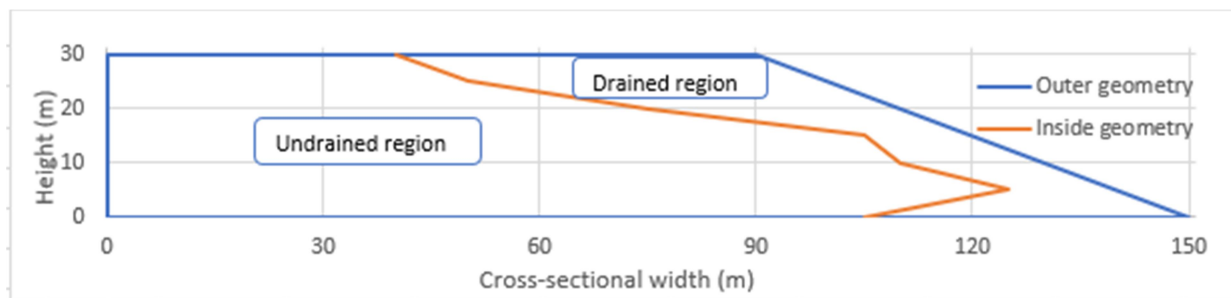
X	Z
0	0
150	0
90	30
0	30
0	0

A variable internal geometry was developed using a spread-sheet which generated varying (X) coordinates at fixed (Z) elevation values. These coordinates demarcated the internal slope boundary between an inner undrained region and an outer drained region. Once the coordinates were generated, they were inserted as inputs, together with the external slope geometry coordinates, into the Rocscience Slide software (i.e. Slide 2 and Slide 3).

Initially, random coordinates for a non-layered internal boundary were generated using a trial Excel spread-sheet. Table 3.2 shows the first internal boundary coordinates generated with Z coordinates separated by 5m increments and randomly generated X coordinates. Figure 3.1 shows the generated 2D slope. For the 3D slope this 2D cross-section was extrapolated 180m along the slope crest.

**Table 3.2: Trial-run internal boundary coordinates**

X	Z
40	30.0
50	25.0
75	20.0
105	15.0
110	10.0
125	5.0
105	0.0

*Figure 3.1: Trial slope*

### 3.2.2 Material parameters

Table 3.3 details the soil properties used in the preliminary models.

**Table 3.3: Preliminary Soil Properties**

Undrained	Drained
Unit weight 20 KN/m <sup>3</sup>	Unit weight 20 KN/m <sup>3</sup>
Cohesion 60 Kpa	Cohesion 0 Kpa
	Friction angle 35°

### 3.2.3 Preliminary results

While 2D results were consistent, software errors were encountered with the 3D analysis. Figure 3.2 shows the preliminary 2D simulation results for the trial slope. A factor of safety of 0.901 was found from the 2D simulation. Figure 3.3, shows the equivalent 3D extrapolated simulation results. A smaller safety value of 0.438 with an irregular slip surface was outputted. The 3D

factor of safety result was observed to be significantly less than the 2D results. This was considered unrealistic and it highlighted an error within the 3D analysis procedure. This error was confirmed at the time by the Rocscience Software Engineer. It was discovered that the Slide 3 software program experienced convergence issues based on the generated internal slope boundaries coordinates and soil property data chosen. It was thus necessary to make modifications to the slope profiling excel spread-sheet and soil properties in order to yield useful results.

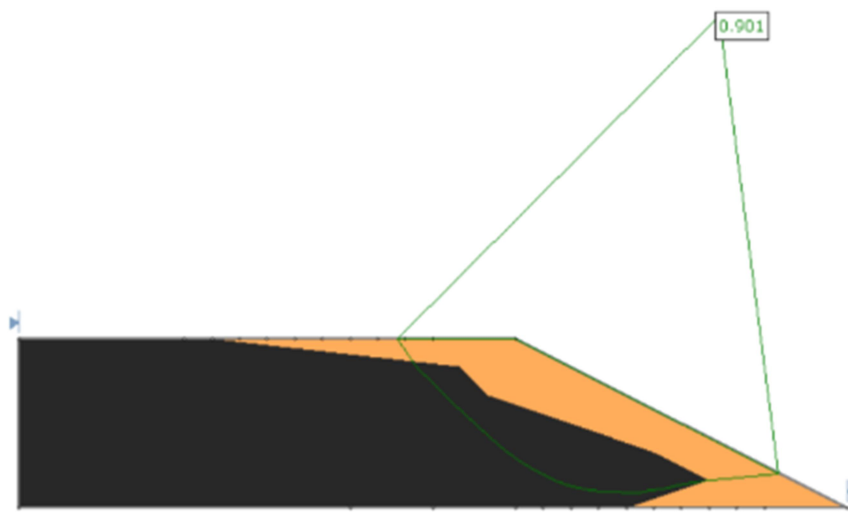


Figure 3.2: Preliminary 2D model analysis result, Courtesy of Slide 2

**FS (Deterministic): 0.438**  
**PF: 100%**

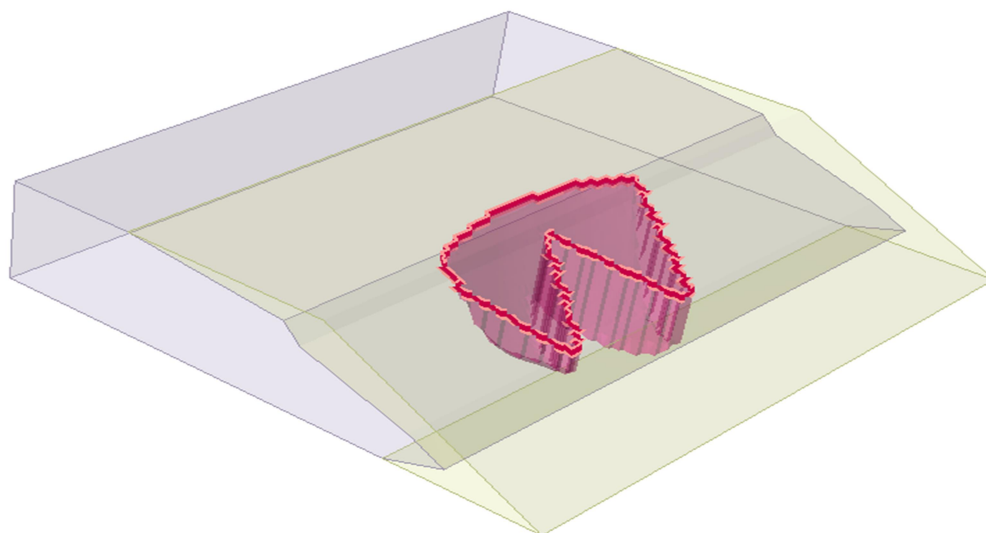


Figure 3.3: Faulty preliminary 3D simulation result, Courtesy of Slide 3

### 3.3 Study models

#### 3.3.1 Internal and external geometry

Following the preliminary modelling, a second Excel spread-sheet was created. The new spread-sheet generated varying stepped internal boundary coordinates. The aim of this internal boundary geometry, separating an undrained region and a drained region, was to mimic the construction sequence of an upstream tailings dam. Descending (Z) elevation values corresponding to the desired layer thickness (i.e. 5m, 3.5m, 2.5m, or 1.5m) were matched with randomly generated (X) values using Excel. For each set of coordinates, each successive (Z) elevation value was given the same (X) value as its predecessor. This was done in order to achieve the desired stepped internal boundary layer geometry. Figure B. 1 and Figure B. 2 in Annexure B shows illustrations of the stepped internal boundary coordinates. Figure 3.4 to Figure 3.7 shows typical cross-sections for each stepped layer configuration.

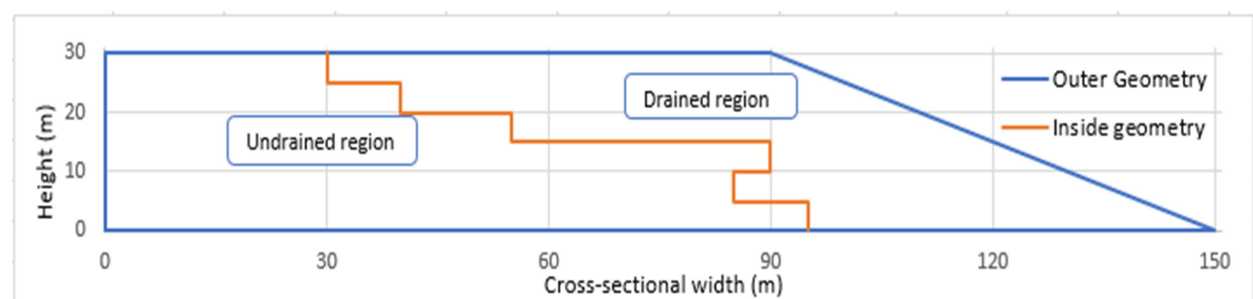


Figure 3.4: Sloped cross section with 5m stepped placement layer

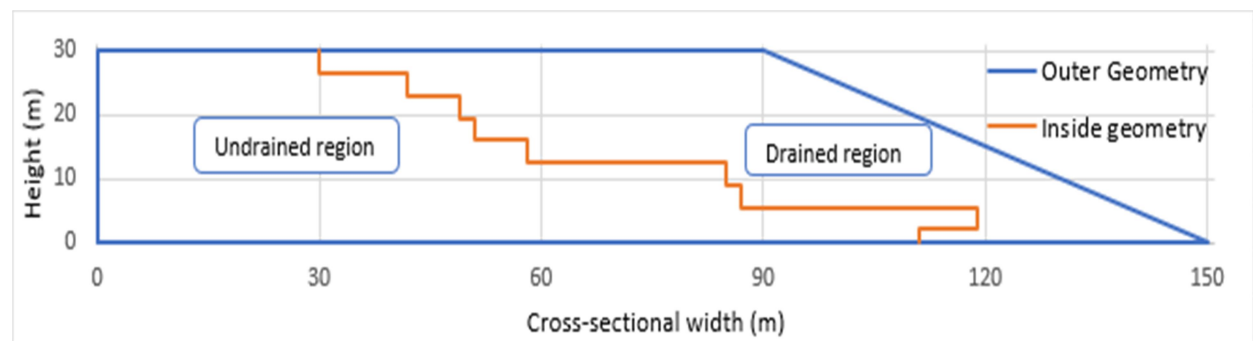


Figure 3.5: Sloped cross section with 3.5 m stepped placement layer

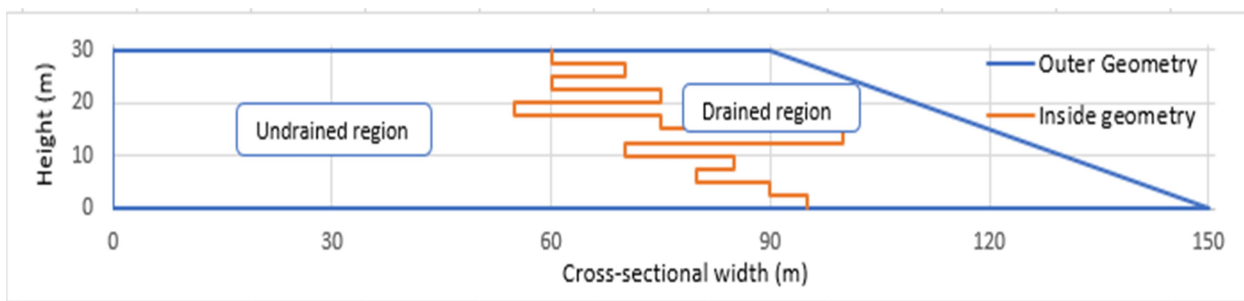


Figure 3.6: Sloped cross section with 2.5 m stepped placement layer

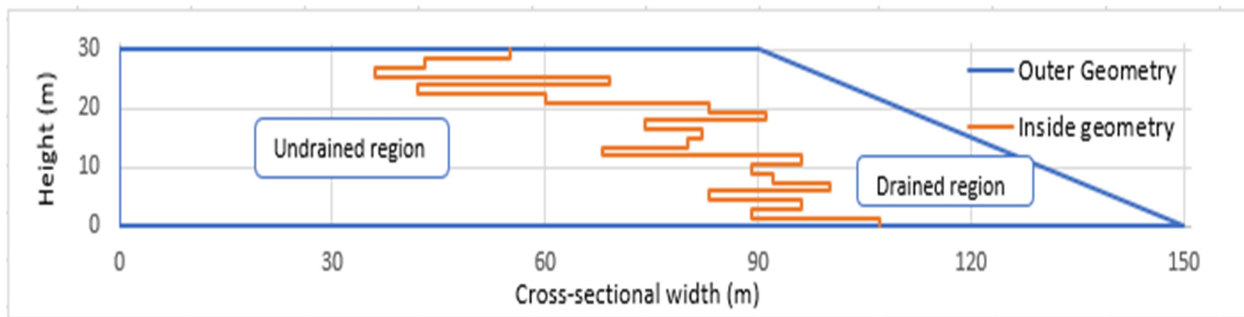


Figure 3.7: Sloped cross section with 1.5 m stepped placement layer

### 3.3.2 Material parameters

The slopes were modelled with an internal undrained region with a unit weight of 20 KN/m<sup>3</sup> and an undrained shear strength of 60 kPa and a friction angle of 0°. No phreatic surface was modelled, however the undrained region was saturated. Furthermore, the external drained region was modelled with a unit weight of 19 KN/m<sup>3</sup>, a friction angle of 31° and cohesion intercept of 10 kPa. A non-zero cohesion intercept was required to avoid convergence issues with Slide 3. These soil parameters are summarised in Table 3.4. These parameters resulted in a factor of safety close to unity.

**Table 3.4: Summary of soil parameters**

	Undrained region	Drained region
Unit weight	20 KN/m <sup>3</sup>	19 KN/m <sup>3</sup>
Cohesion	60 kPa	10 kPa
Friction angle	0	31°

### 3.3.3 Probabilistic material parameters

Table 3.5 shows the statistical distribution used for the two slope materials. For the probabilistic analysis the Latin Hypercube Sampling technique with 1000 samples was used. Latin Hypercube simulation is dependent on previously sampled data. It involves the equal subdivision of cumulative density functions before choosing random data in each subdivision (Menčík, 2016). With this method, a better representation of the expected distribution is acquired when receiving the output parameters. Additional information on this method can be found in Annexure C.

The material statistics values, shown in Table 3.5, were obtained from suggested values compiled by Rocscience which are provided in Figure A. 1 in Annexure A. For the undrained region, since a mean cohesion of 60 kPa was chosen, the probabilistic simulation would run 1000 simulations for each individual slope, with a unique cohesion being sampled between 42 kPa and 78 kPa using Latin Hypercube Sampling. Similarly, for the Drained region's friction angle, the Latin Hypercube Sampling would select a unique friction angles between 25° and 37° for the 1000 simulations of each slope.

**Table 3.5: Varied Parameters**

Soil property	Distribution	Standard deviation
Undrained region – (Cohesion)	Normal distribution	6 (Relative Min: -18, Relative Max: 18)
Drained region – (Friction angle)	Normal distribution	2 (Relative Min: -6, Relative Max: 6)

### 3.3.4 2D Models

External slope coordinates were used together with the stepped internal boundary coordinates to generate 2D models in Slide 2D.

### 3.3.5 3D Extrapolated Models

Similar to the 2D modelling procedure, the external slope coordinates were used with stepped internal boundary coordinates, corresponding with the 2D model counterparts. These 2D cross-section were extrapolated (or extruded) for a longitudinal distance of 180 metres in order to generate an equivalent 3D extrapolated model. Figure 3.8 shows a typical 3D Extrapolated model generated using the Slide 3 software program.

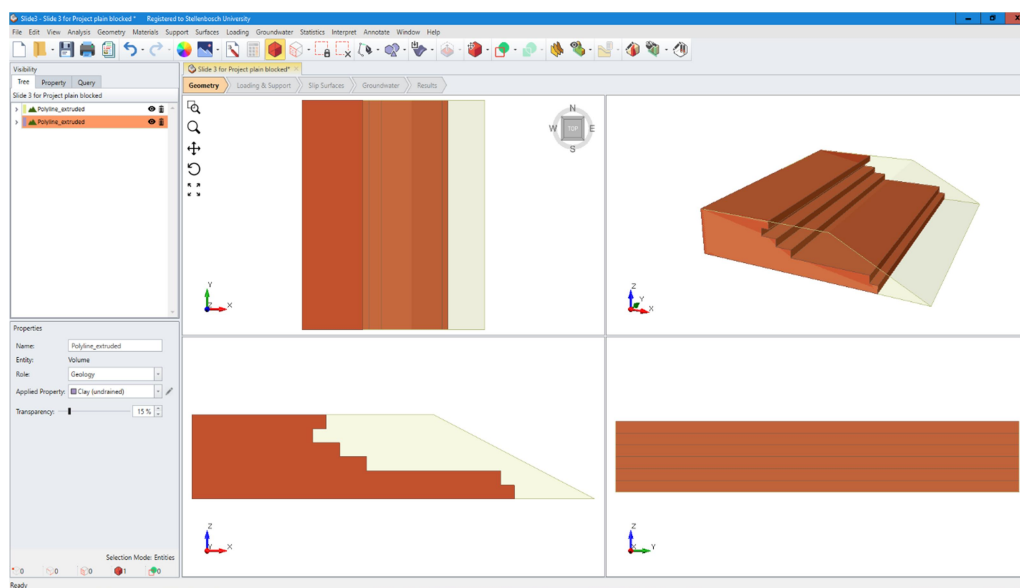


Figure 3.8: 3D Extrapolated slope illustration, Courtesy of Slide 3

### 3.3.6 3D Composite Models

Three 2D and 3D extrapolated models made up a set, with each numbered (i.e. 1, 2, and 3). Composite models were then created by stitching together three component cross-sections each extrapolated by 60 metres for a total longitudinal slope length of 180 metres. The ordering of the section was varied to mimic variable conditions along a slope. The component cross sections for each set were varied three times in the following sequences i.e. (1, 2, 3); (1, 3, 2); and (2, 1, 3). These produced three different composite sections for each set. Due to symmetry, no further combinations were used. An example is given in Figure 3.9.

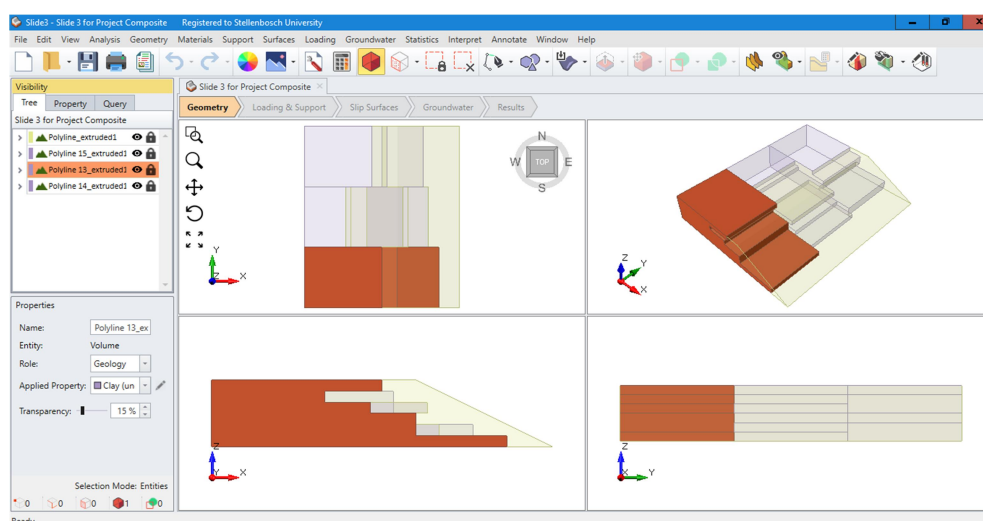


Figure 3.9: 3D composite slope illustration

### **3.3.7 Limit equilibrium method and search algorithm**

The Morgenstern and Price's method and Spencer's method were used for analysis of all three slope models (i.e. 2D, 3D Extrapolated and 3D Composite). For the Morgenstern and Price method, the interslice force function had to be selected as opposed to the Spencer method. The default half-sine interslice force function was chosen.

A deterministic and probabilistic slope stability analysis was done for all three analysis approaches (i.e. 2D, 3D Extrapolated and 3D Composite). For the 2D simulations, the Auto-Refine Search method was used to find each slope's critical surface. The Auto-Refined search method was chosen simply due to it being the default method of choice during the initial stages. Due to the lack of an Auto-Refine Search Method within Slide 3, the Cuckoo Search Method was used. Details on the Auto-Refine and Cuckoo search methods are given below:

#### **I) Auto Refined Search**

This is a method used in optimizing the identification of the critical slip surface location. The method is an iterative process which uses the results acquired in one iteration as a means of reducing the search area for the lowest factor of safety results. Initially the slope section undergoes a division process. For each division, circles are generated from which the factor of safety for each division is determined. After the average factor of safety for each division has been determined, the first iteration phase ends. By analysing the outputs in each division and determining the regions with the lowest factors of safety, the next iterations are carried out with a greater focus on dividing the newly determined critical regions. This is repeated until the target number of iterations has been reached and the lowest factor of safety has been established. (RocScience, 2021).

#### **II) Cuckoo Search**

According to RocScience (2021), this method is a very quick and efficient means of locating a slopes critical slip surface. The method requires no user inputs in order to generate trial surfaces in the search of critical slip surfaces and regions. Cuckoo Search uses output results of previously found slip surfaces for the location of new potentially more critical failure surfaces. An algorithm is used to initialise a fixed number of valid solutions ( $N$ ) and iterations ( $I_{max}$ ) that are dependent on the complexity of the problem as well as the solution vectors. Through an iteration process, solution vectors are determined and compared to proceeding solution vectors from the following set of iterations. If a better solution is found, the original

solution vector is replaced (RocScience, 2021). This is done until the most critical slope analysis outcome is found (i.e. lowest factor of safety).

### 3.3.8 Results capturing

Table 3.6 gives summary of the results acquired by each slope stability analysis approach.

Table 3.7 gives the number of scenarios modelled per layer thickens

**Table 3.6: Results obtained**

2D Slope analysis	3D Extrapolated slope analysis	3D Composite slope analysis
2D Deterministic Factor of Safety ( $F_{2D}$ )	3D Deterministic Factor of Safety ( $F_{EXT}$ )	3D Deterministic Factor of Safety ( $F_{COMP}$ )
2D Probabilistic Factor of Safety	3D Probabilistic Factor of Safety	3D Probabilistic Factor of Safety
2D Probability of Failure	3D Extrapolated Probability of Failure	3D Composite Probability of Failure

**Table 3.7: Simulation scenarios**

Scenario	Name	Total slopes analysed for 2D, 3D Extrapolated and 3D Composite models
1	3 thick (5m)	135
2	2 thick (5m)	135
3	3 thick (2.5m)	180
4	4 thick (2.5m)	180
5	4 thick (1.5m)	192
6	5 thick (1.5m)	96
7	3 thick (3.5m)	114

Each scenario name consisted of a minimum wall thickness value that was used during the generation of the stepped internal boundary layer coordinates. The wall thickness was selected from a range between the minimum value which was specified and the maximum value of 12m. Alongside the minimum wall thickness value, the term "thick" was paired with a number in brackets reflecting the thickness of stepped internal boundary layers. For instance, the scenario named [4 thick (2.5m)] would contain slopes with 2.5m stepped internal boundary layers generated using wall thickness values ranging between 4 metres and 12 metres. Table A. 1 In the annexure gives a full guideline of the research results Excel Spread-sheets.

### 3.3.9 Run times

All models were manually inputted as Slide 2 and 3 do not support batch processing. Table 3.8 gives the total number of simulations completed and associated run times for each simulation. To reduce the total time to obtain results, 2D and 3D Extruded simulations were run simultaneously using two computers. On each computer a 2D and 3D Extrapolated simulation was carried out. For the Composite slope analysis, 3 computers were used, with each computer running a 3D composite simulation. This was done back and forth until all 1032 slope models had been analysed both deterministically and probabilistically. On average it took 1 hour to generate, model, simulate and record 45 2D and 3D Extrapolated models using the two computers. For the 3D Composite models, it took an average 1 hour and 15 minutes to generate, model, simulate and record 45 slope models using 3 computers.

**Table 3.8: Study models initial summary**

	2D Slope analysis	3D Extrapolated slope analysis	3D Composite slope analysis
<b>Total number of slope stability analysis simulations</b>	1032	1032	1032
<b>Average run time (for one simulation)</b>	10 seconds	3.5 minutes	4.5 minutes

### **3.3.10 Methodology summary**

In summary, Slide 2 and Slide 3 software programs from Rocscience was used to analyse 2D models, 3D extrapolated models made from 2D extrapolated sections and, 3D composite models consisting of three merged 2D extrapolated slope sections. 1032 slopes were analysed using each of the three analysis models. Different internal boundary geometries were used separating a drained and undrained region of the slope models. The internal boundaries were of a stepped nature, and were generated using Excel. Four stepped internal boundary layer thicknesses were used (5m, 3.5m, 2.5m and 1.5m). Lastly, Deterministic and Probabilistic analysis were run for each slope using the Morgenstern and Price and, Spencer method.

## Chapter 4: Results, Analysis and Discussion

### 4.1 Introduction

This chapter presents the results obtained together with the analysis and research findings. The results include slope stability analysis for the 2D slope models, 3D extrapolated models as well as the 3D composite models. This section only considers factors of safety. During the analysis the software computed many 3D probabilities of failure with values of zero. As a result, there was not enough data to make substantial probability of failure comparisons between the 3 analysis approaches.

### 4.2 Presentation of typical slip surfaces

The following section gives the typical slip surfaces obtained from the slope stability analysis results for the stepped internal boundary between the undrained region and drained region.

#### 4.2.1 2D Slopes

Figure 4.1 to Figure 4.4 shows typical 2D analysis results which were obtained for the four main slopes groups which were generated (i.e. slopes with either 5m, 3.5m, 2.5m, or 1.5m stepped internal boundary layers). For all the slip surfaces, it is observed that critical slip surfaces predominantly cut through undrained region exiting low at the toe.

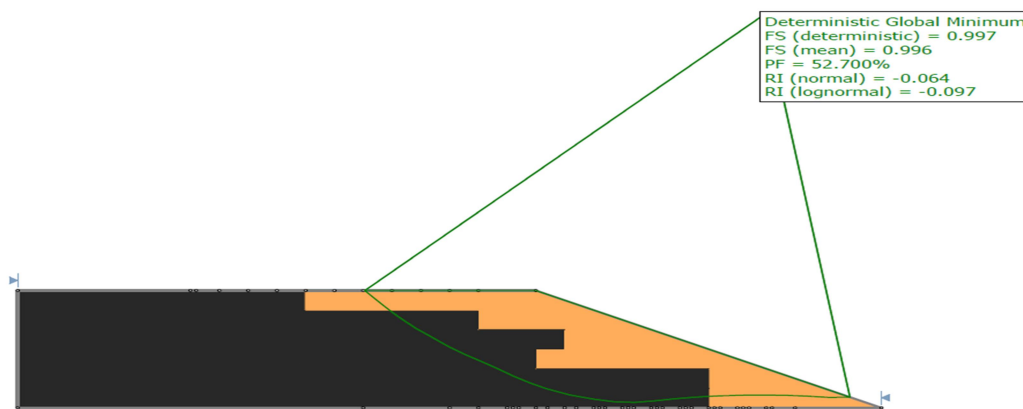


Figure 4.1: 2D Slope cross-section with 5m stepped placement layer

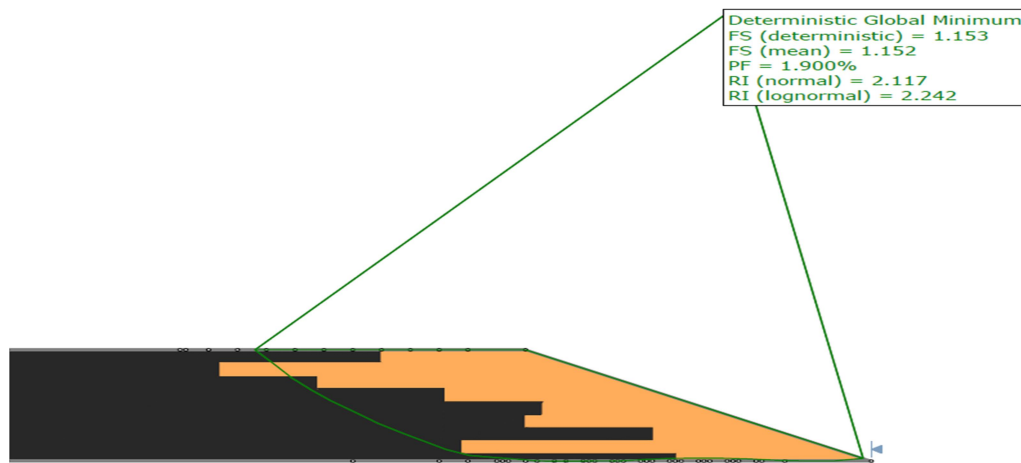


Figure 4.2: 2D Slope cross section with 3.5 m stepped placement layer

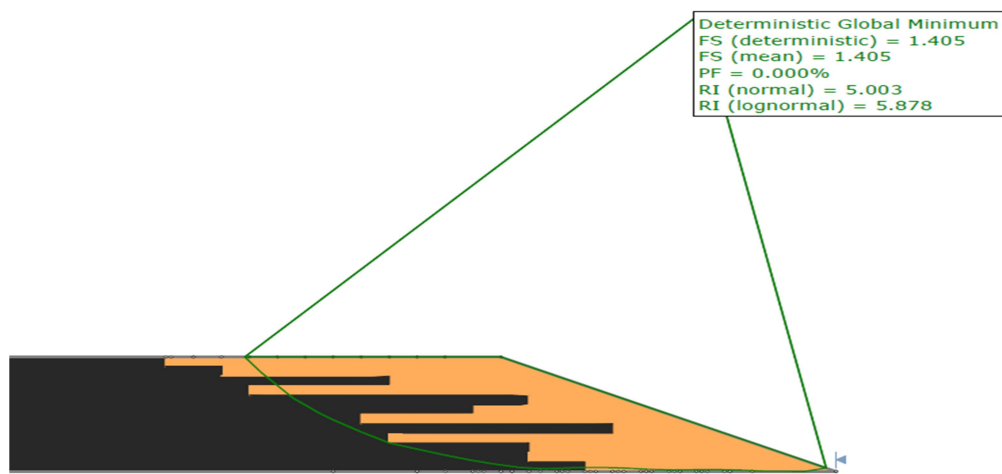


Figure 4.3: 2D Slope cross section with 2.5 m stepped placement layer

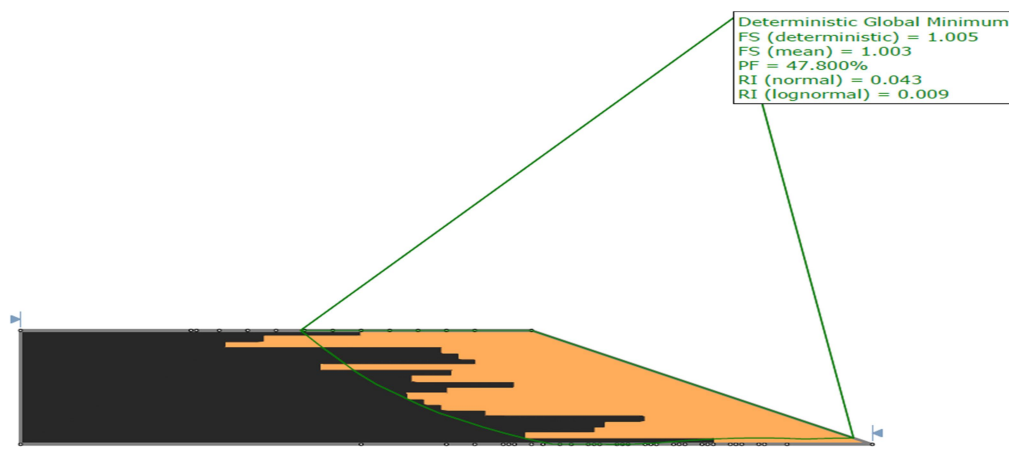


Figure 4.4: 2D Slope cross section with 1.5 m stepped placement layer

#### 4.2.2 3D Extrapolated Slopes

Figure 4.5 shows the slope analysis results for a typical 3D extrapolated slope model with 5m stepped internal boundary layer thicknesses. Similar slip surfaces were obtained for all internal boundary thicknesses (i.e. for 3.5 m, 2.5 m and 1.5 m stepped internal boundary layers).

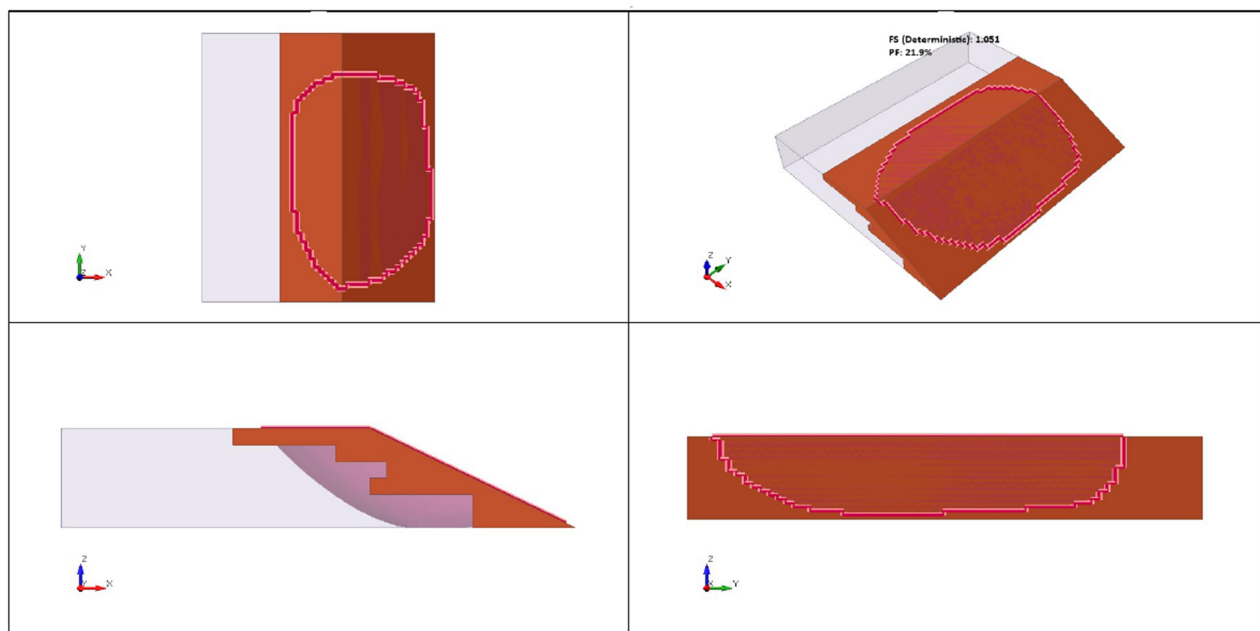


Figure 4.5: Sloped cross section with 5m stepped placement layer

#### 4.2.3 3D Composite Slopes

Figure 4.6 shows the slope analysis results for a typical 3D composite slope model with 5m stepped internal boundary layer thicknesses. Similar slip surfaces were obtained for all internal boundary thicknesses (i.e. for 3.5 m, 2.5 m and 1.5 m stepped internal boundary layers).

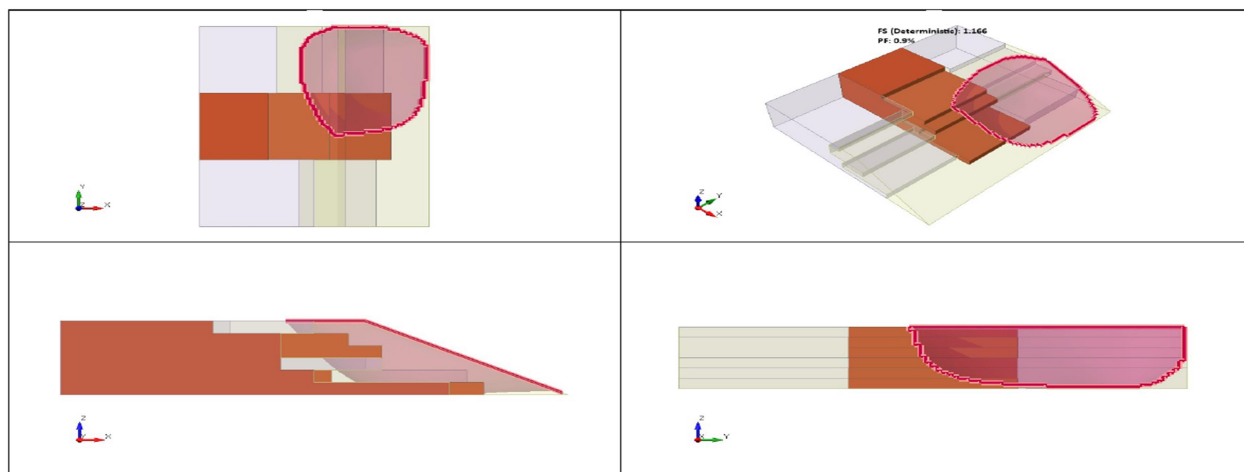


Figure 4.6: Sloped cross section with 5m stepped placement layer

### 4.3 Comparison of Analysis methods FOS results

#### 4.3.1 Morgenstern and Price FOS, and Spencer's FOS comparison

Figure 4.7 to Figure 4.9 show the results obtained from the comparison of the deterministic factor of safety values obtained using The Morgenstern and Price method, and Spencer's method for the 2D, 3D extrapolated and 3D composite slope sections.

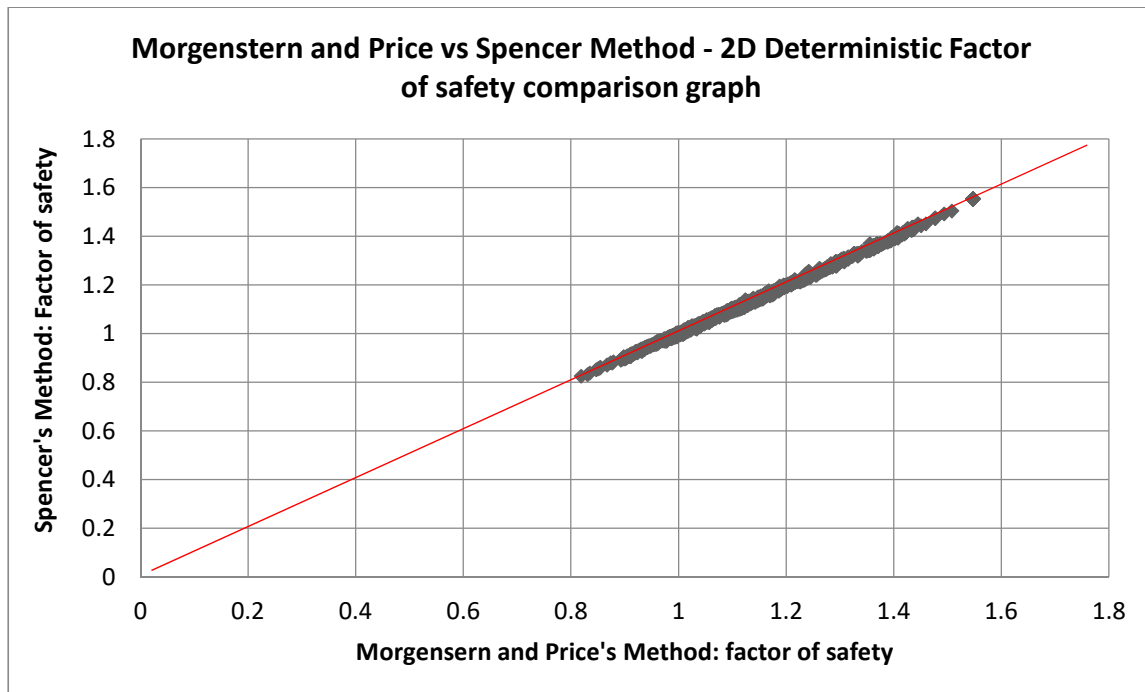


Figure 4.7: 2D deterministic FOS comparison

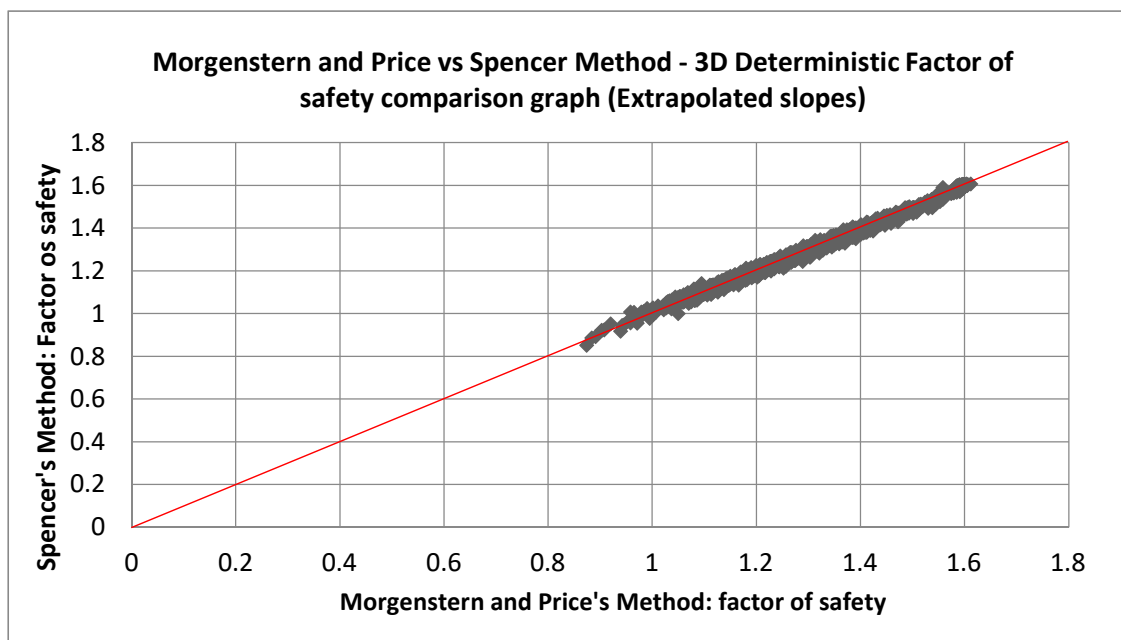


Figure 4.8: 3D extrapolated deterministic FOS comparison

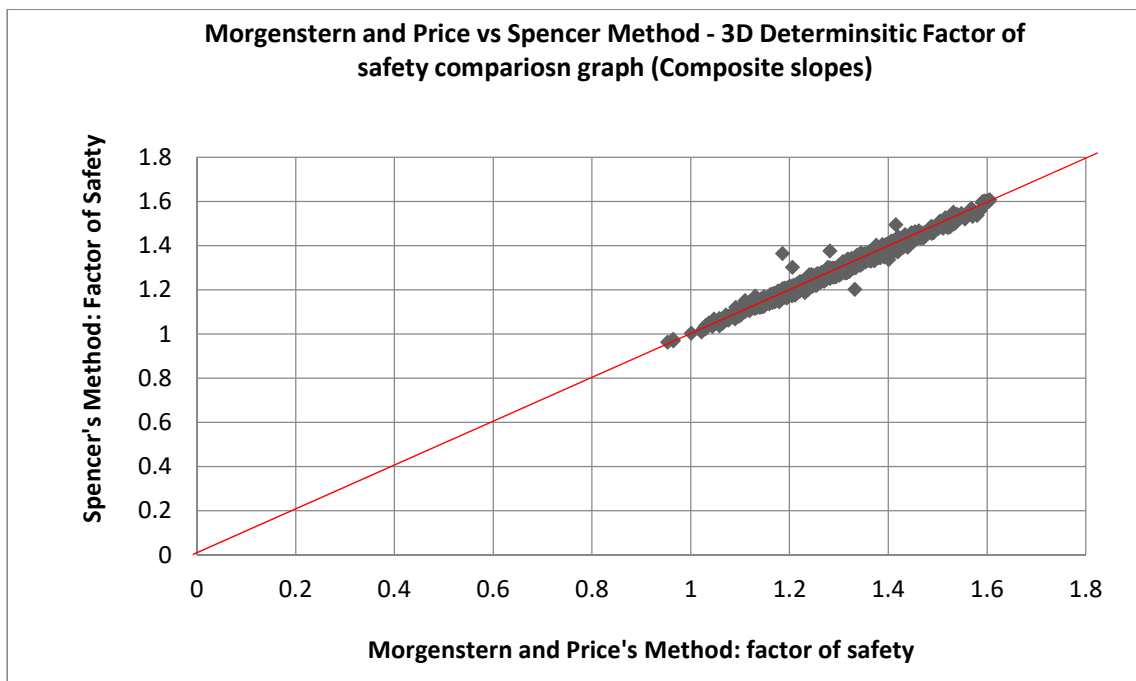


Figure 4.9: 3D composite deterministic FOS comparison

Figure 4.7 to Figure 4.9 show that the factor of safety results for the 2D, 3D extrapolated and 3D composite slopes show close agreement between the two limit equilibrium methods. In Figure 4.9, a few outliers out of the 816 3D composite models run can be seen. Reasons for this discrepancy is likely the result of dissimilar critical slip surfaces being obtained by the two limit equilibrium methods as 3D composite models incorporated variability along the slope length. A close relationship was also observed for the average factor of safety determined from the probabilistic analysis (Figure A. 2 to Figure A. 4 in Annexure A). Due to the similarities in results for Morgenstern and Price method and Spencer's method, Spencer's method was chosen as the primary method of focus for further analysis.

#### 4.3.2 Comparison between Auto Refine Method versus Cuckoo Search Method

Due to the use of Cuckoo Search method in the 3D analysis for the location of the critical slip surface as opposed to the Auto refined Search for the 2D analysis, a comparison between the two methods was done. This comparison was done for 2D results. 60 deterministic factor of safety values, using Spencer's Method, were sampled from the overall results. 15 samples were each taken from the 4 major stepped layer categories (i.e. 5m, 3.5m, 2.5m and 1.5m) to make up the 60 samples. These samples were then reanalysed using Slide 2 with the Cuckoo slip surface searching method. Figure 4.10 shows the comparison plot which was obtained.

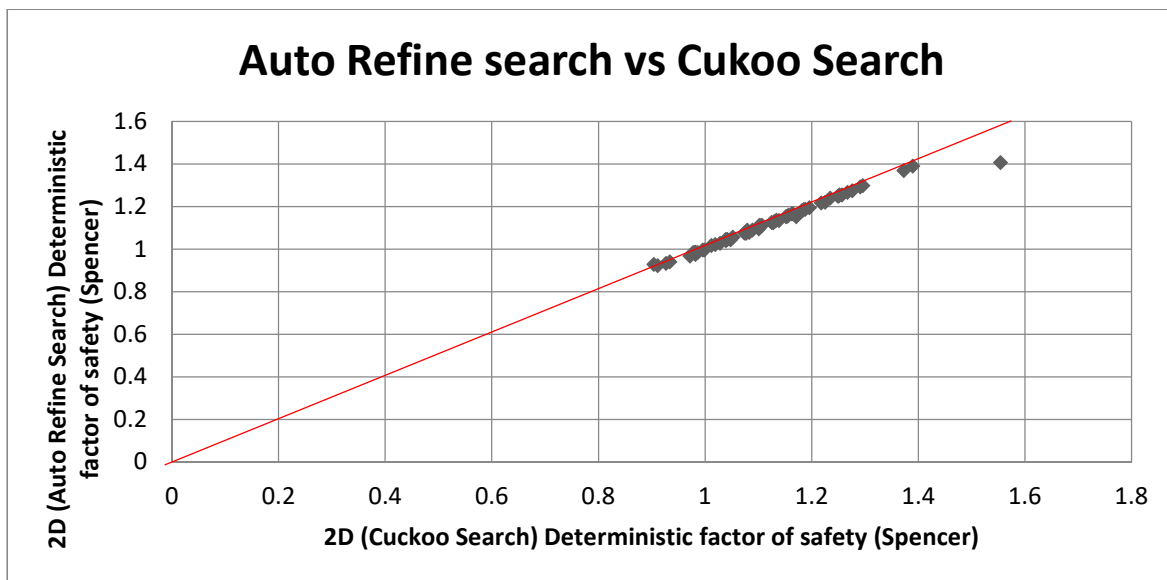


Figure 4.10: Auto Refine Search versus Cuckoo search Method results using Slide 2

The factor of safety values obtained using the two slip surface search methods yielded similar results as can be observed in Figure 4.10. An outlier can be spotted on the graph which yields a cuckoo search factor of safety of 1.554 and an equivalent Auto Refine safety factor of 1.406. Reasons for this might be due to the Cuckoo search method not being able to locate a more critical slip surface during its iterative search for more critical vector solutions. This could have been caused by the stepped internal boundary being too complex. Nevertheless, these results show that it was acceptable to use the Auto refine method instead of the Cuckoo search method for the 2D analysis.

#### 4.4 Overall frequency screening of results

##### 4.4.1 Abnormal value checks

Upon completion of the 1032 results for the 2D, 3D extrapolated and 3D composite slopes, FOS values were plotted on a histogram (Figure 4.11). A spike in FOS values around 1.6 was observed for 2D and 3D extrapolated sections. Upon closer review of the results, it was observed that for certain slopes, unusually high 3D factor of safety values ( $F_{EXT}$ ) are obtained with relatively lower 2D slope safety factor ( $F_{2D}$ ). Figure B. 3 in annexure B shows a typical data recording output containing an abnormal factor of safety result. These were considered to be erroneous and removed from the dataset. This eliminated 216 scenarios. Thus, a total of 816 slopes were analysed for the 2D, 3D extrapolated and 3D composite slope models (see Table 4.1).

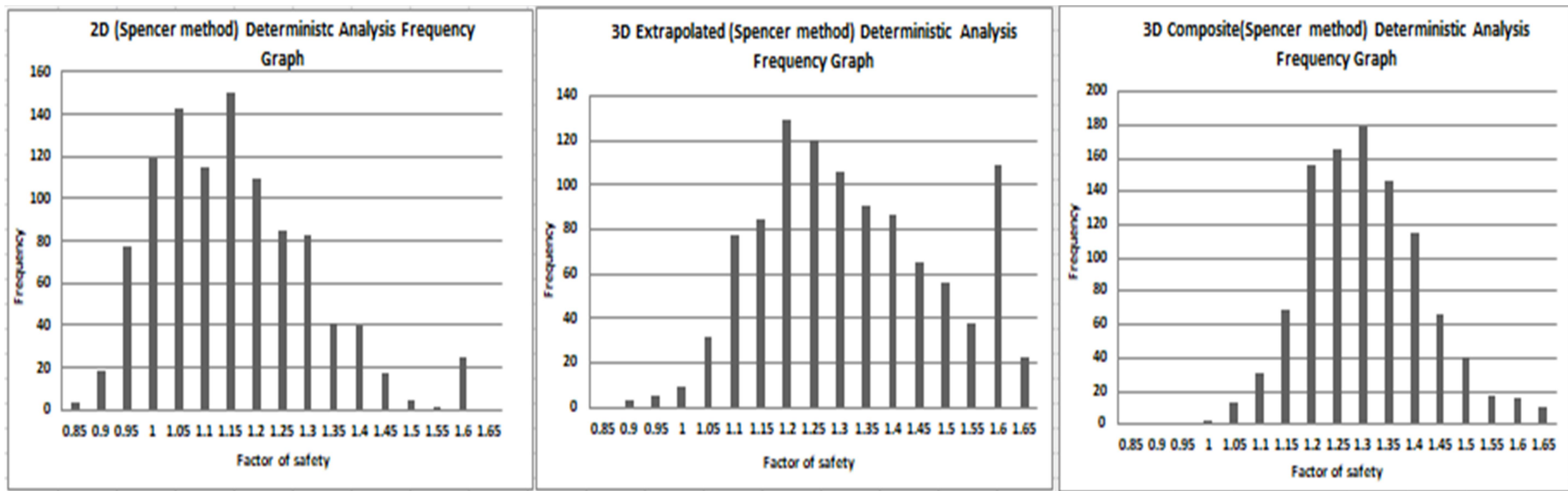


Figure 4.11: 2D, 3D Extrapolated and 3D Composite factor of safety frequency graph with tail spike

Table 4.1: Study models final summary

	2D Slope analysis	3D Extrapolated slope analysis	3D Composite slope analysis
Total number of slope stability analysis simulations	816	816	816
Total number of slope stability analysis sets	272	272	272

#### 4.4.2 Reduced data set check

Figure 4.12 shows the results of the frequency distribution graphs for the 816 remaining subsequent slope models after the exclusion of outliers. For the 2D results shown in Figure 4.12, a lognormal frequency distribution skewed towards the left was observed. The mean frequency FOS for the 2D results was 1.11. FOS values for 3D extrapolated models had a right skewed distribution with a mean FOS of 1.28. For 3D composite models, the distribution was more normal distribution with a mean FOS of 1.27.

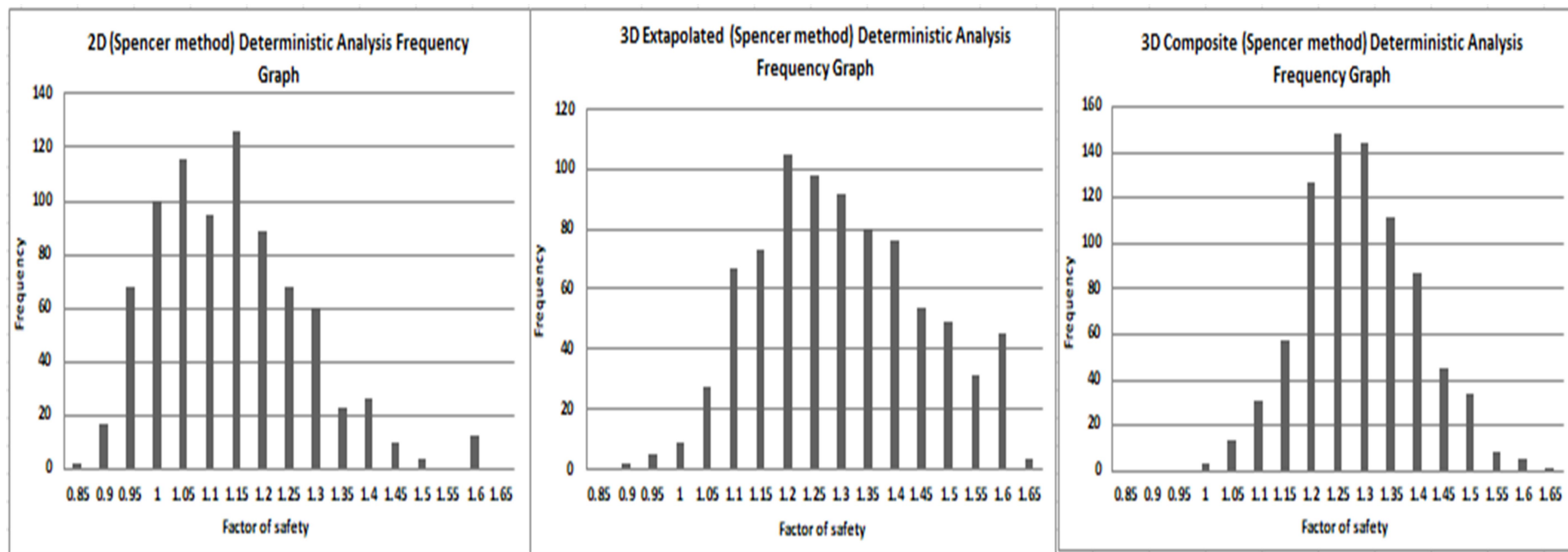
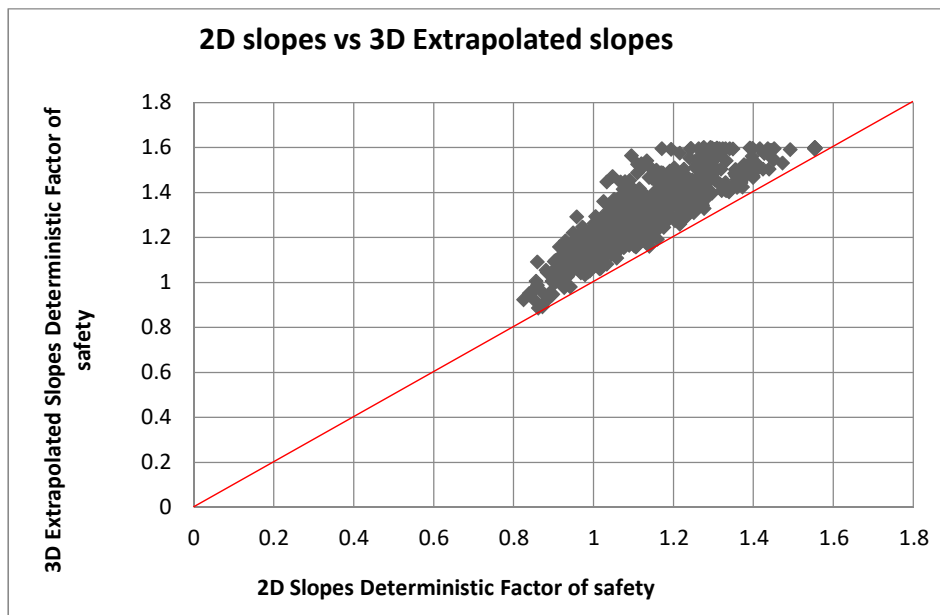


Figure 4.12: 2D, 3D Extrapolated and 3D Composite factor of safety frequency graph with controlled spikes

#### 4.4.3 Overall $F_{2D}$ versus $F_{EXT}$ comparative plot

Figure 4.13 shows a scatter plot comparing factor of safety for the 2D slopes and companion 3D extrapolated slopes. All 3D extrapolated FOS values were greater than their respective 2D FOS counterparts. This is also evident from the mean frequencies highlighted earlier.



*Figure 4.13: 2D slopes versus 3D extrapolated slopes comparison*

The average percentage difference between the 3D extrapolated FOS values and the corresponding 2D FOS values was 15%. A minimum and maximum percentage difference of 0% and 44% was observed between the two methods respectively. Table 4.2 shows a summary of the percentage differences which were experienced between the 3D extrapolated FOS values and 2D FOS values. The highest percentage difference was between (10% and 20%) with 57% of the slopes analysed falling within this category.

**Table 4.2: Summarised 2D versus 3D comparison data**

Percentage difference category	0% - 10%	10% - 20 %	20% - 30%	30 % - 45%
Percentage out of 816 slope stability simulations	22%	57%	18%	3%

## 4.5 Analysis of the ideal and worst-case

In practice, after determination of the slope's soil parameters, the analysis results would have been similar to the results obtained from the single analysis of  $F_{2D}$  and  $F_{EXT}$ . However, the actual conditions would have been similar to those of  $F_{COMP}$  which are made up of more than one cross section. The  $F_{COMP}$  value incorporates the possibility of a lower factor of safety in a neighbouring unsampled cross-section being present. A slope will naturally collapse where it is weakest, and it is possible that this part was not sampled. To accommodate this, best practices dictate factors of safety be included to reduce the potentially dangerous circumstances that may arise.

### 4.5.1 $F_{EXT}$ compared to $F_{COMP}$

Consideration is thus first given to comparing  $F_{EXT}$  values to  $F_{COMP}$  values. If the 3D extrapolated factor of safety ( $F_{EXT}$ ) was higher than the corresponding 3D composite Factor of safety ( $F_{COMP}$ ), the analysis would be unsafe. An ideal case as well as a worst-case are considered.

An unsafe analysis for the ideal case would occur if the weakest slope section was sampled (i.e. slope that yielded lowest  $F_{EXT}$ ) and the strongest composite model existed (i.e. slope that yielded the highest  $F_{COMP}$ ). Figure 4.14 illustrates an unsafe analysis for the ideal case.

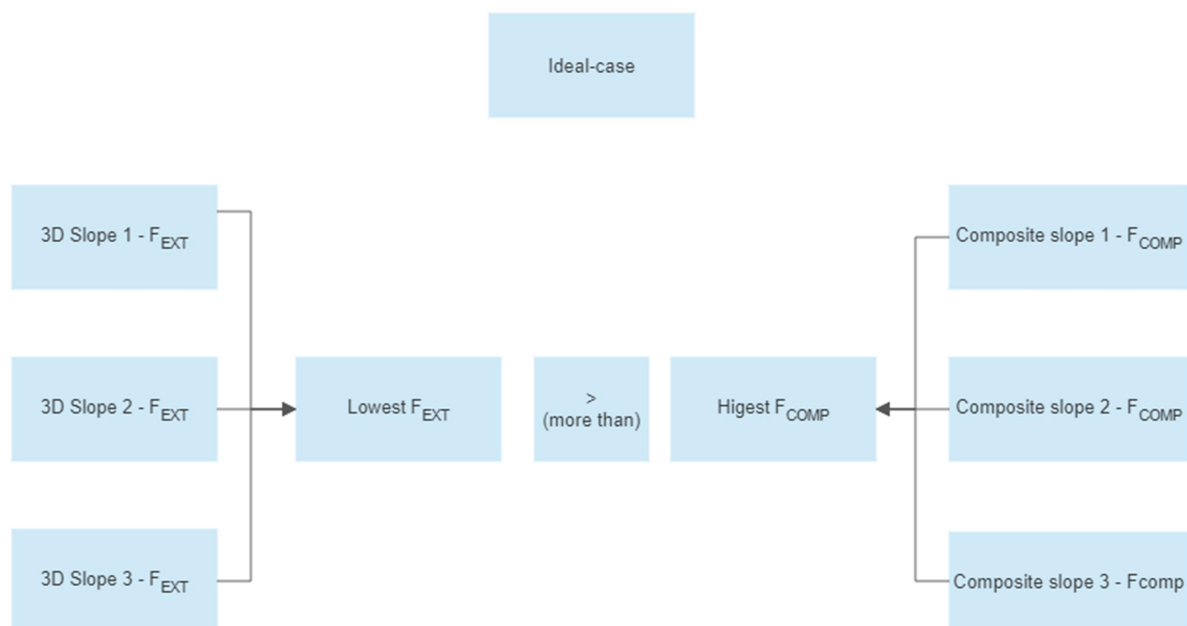
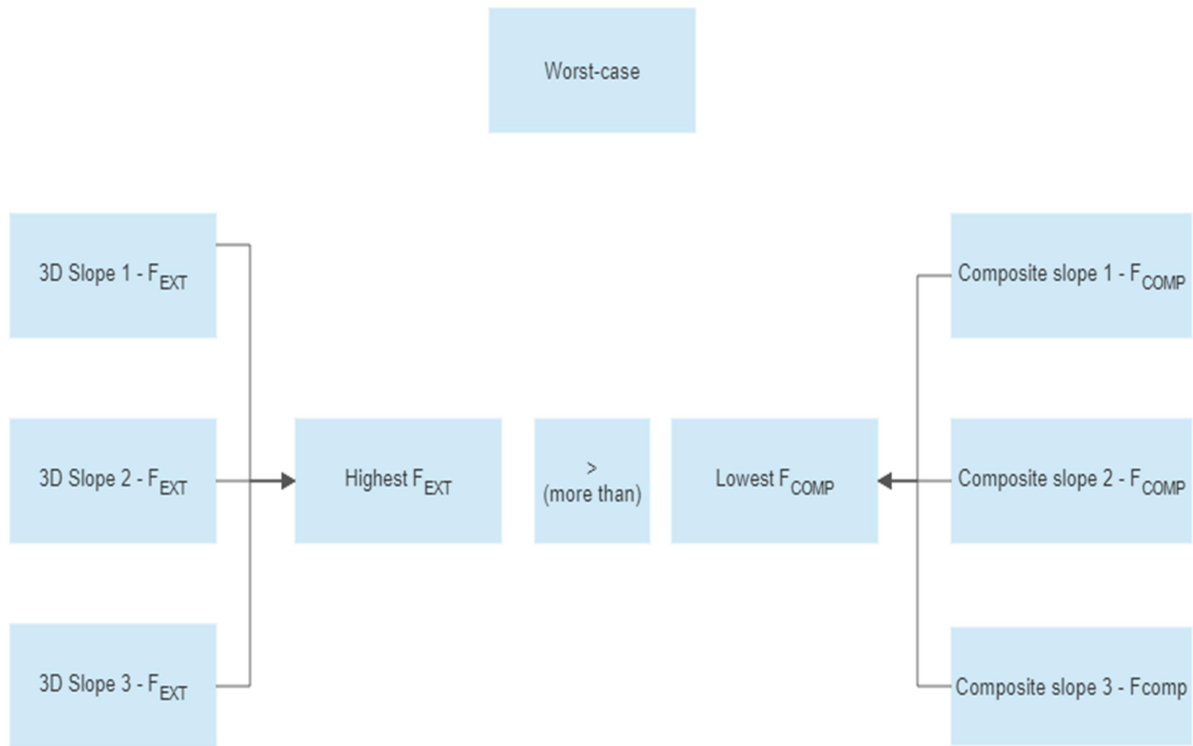


Figure 4.14: Unsafe analysis set for ideal case for 3D analysis

An unsafe analysis for the worst-case would occur if the strongest slope section was sampled (i.e. slope that yielded the highest  $F_{EXT}$ ) and the weakest composite model existed (i.e. slope that yielded the lowest  $F_{COMP}$ ). Figure 4.15 illustrates an unsafe analysis for the worst-case.



*Figure 4.15: Unsafe analysis set for worst-case for 3D analysis*

A comparison was thus done between the lowest  $F_{EXT}$  and highest  $F_{COMP}$  as well as for the highest  $F_{EXT}$  and lowest  $F_{COMP}$ . This was done for each set of the 816 slope simulations. Each set consisted of three 2D, 3D extrapolated models and 3D composite models created through the stitching of three component cross-sections. The results for the 816 slope stability simulations show that for an ideal case when the weakest  $F_{EXT}$  value was compared to the strongest  $F_{COMP}$  value, 1% of the comparisons lead to an unsafe analysis. However, for the worst-case, comparing the strongest  $F_{EXT}$  value to the weakest  $F_{COMP}$  value, 99% of the analysis were found to be unsafe. This shows the risk of using extrapolation methods especially when the section of the slope that is analysed is not the weakest.

Table 4.3 shows the results which were obtained from the Ideal and worst case following the comparisons of the appropriate  $F_{EXT}$  and  $F_{COMP}$  values. The results for the 816 slope stability simulations show that for an ideal case when the weakest  $F_{EXT}$  value was compared to the

strongest  $F_{COMP}$  value, 1% of the comparisons lead to an unsafe analysis. However, for the worst-case, comparing the strongest  $F_{EXT}$  value to the weakest  $F_{COMP}$  value, 99% of the analysis were found to be unsafe. This shows the risk of using extrapolation methods especially when the section of the slope that is analysed is not the weakest.

**Table 4.3: Safety comparison for  $F_{EXT}$  compared to  $F_{COMP}$**

Ideal-case		Worst-case	
Total number of slope stability analysis	816	Total number of slope stability analysis	816
Total slope stability sets	272	Total slope stability sets	272
Unsafe sets ( $\min F_{EXT} > \max F_{COMP}$ )	2	Unsafe sets ( $\max F_{EXT} > \min F_{COMP}$ )	270
Safe ( $\max F_{COMP} > \min F_{EXT}$ )	270	Safe ( $\min F_{COMP} > \max F_{EXT}$ )	2
Unsafe	1%	Unsafe	99%

#### 4.5.2 $F_{2D}$ compared to $F_{COMP}$

A comparison between  $F_{2D}$  and  $F_{COMP}$  was done for the 816 simulations. With this comparison, the effects of 2D would be the main priority; similar to current practice in the geotechnical industry. If the 2D factor of safety ( $F_{2D}$ ) was higher than the 3D composite Factor of safety ( $F_{COMP}$ ) being compared an unsafe analysis was present. Similar to the previous section, a worst-case and ideal-case was analysed.

An unsafe analysis for the ideal-case would occur if the weakest slope section was sampled (i.e. slope that yielded lowest  $F_{2D}$ ) and the strongest composite model existed (i.e. slope that yielded the highest  $F_{COMP}$ ). Figure 4.16 illustrates an unsafe analysis for the ideal-case.

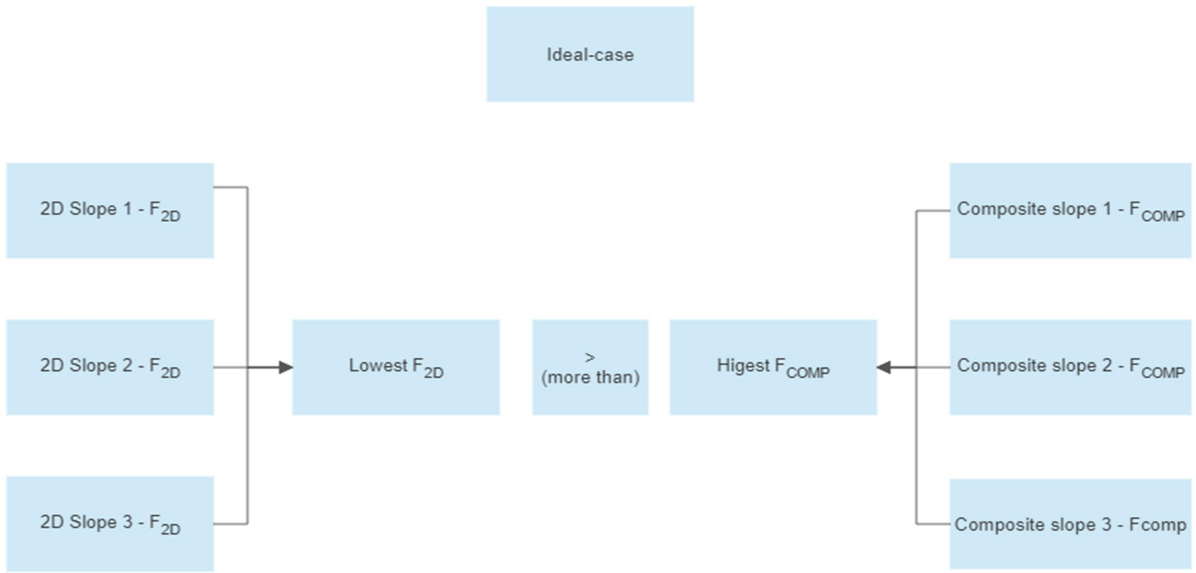


Figure 4.16: Unsafe analysis for ideal case for 2D analysis

An unsafe analysis for the worst-case would occur if the strongest slope section was sampled (i.e. slope that yielded the highest  $F_{2D}$ ) and the weakest composite model existed (i.e. slope that yielded the lowest  $F_{COMP}$ ). Figure 4.17 illustrates an unsafe analysis for the worst-case.

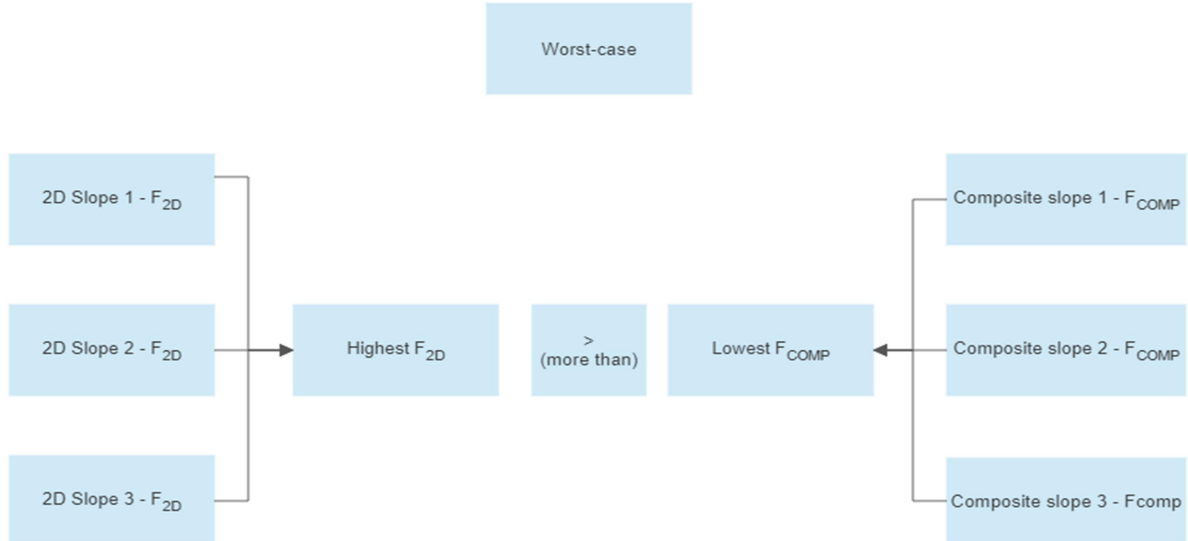


Figure 4.17: Unsafe analysis for worst-case for 2D analysis

A comparison was thus done for between the lowest  $F_{2D}$  and highest  $F_{COMP}$  as well as for the highest  $F_{2D}$  and lowest  $F_{COMP}$ . This was done for each set of the 816 slope simulations. Table 4.4 shows the results which were obtained from the ideal and worst-case following the comparisons of the appropriate  $F_{2D}$  and  $F_{COMP}$  values.

**Table 4.4: Safety comparison for F<sub>2D</sub> compared to F<sub>COMP</sub>**

	Ideal-case		Worst-case
Total slope stability sets	272	Total slope stability sets	272
Unsafe sets (min F <sub>2D</sub> > max F <sub>COMP</sub> )	0	Unsafe sets (max F <sub>2D</sub> > min F <sub>COMP</sub> )	120
Safe (max F <sub>COMP</sub> > min F <sub>2D</sub> )	272	Safe sets (min F <sub>COMP</sub> > max F <sub>2D</sub> )	152
Unsafe	0%	Unsafe	44%

The results for the 816 slope stability simulations show that for an ideal-case when the weakest F<sub>2D</sub> value was compared to the strongest F<sub>COMP</sub> value, there were no unsafe analysis executed. However, when the worst-case was looked at through comparing the strongest F<sub>2D</sub> value to the weakest F<sub>COMP</sub> value, 44% of the analysis were found to be unsafe using the extrapolation method.

These results show that when the ideal section is sampled during site investigation and used to conduct 2D slope stability analysis, the results for the slope stability analysis performed are safe. In instances where non-critical sections are sampled and used for conducting 2D slope stability analysis, the chances of conducting unsafe analysis do exist (i.e. 44%). However, the chances of conducting unsafe analysis are significantly reduced (by 55%) as compared to when 3D slope stability analyses are done using 3D slopes created from extrapolated sections.

## 4.6 Analysis using coefficient of variation

### 4.6.1 F<sub>EXT</sub> and F<sub>COMP</sub> difference versus coefficient of variation graph

A graph showing the average difference between F<sub>EXT</sub> and F<sub>COMP</sub> values that resulted in safe and unsafe scenarios, for the ideal, average and worst cases, was plotted against the coefficient of variation. This can be seen in Figure 4.18. The coefficient of variation is a measure of the spatial variability inherent to a given composite slope. The higher the value the greater variation in the conditions between the three sections making up the composite slope.

The coefficient of variation for each set was determined using the formula:

$$\text{Coefficient of variation} = \frac{\text{Standard deviation for } F_{\text{EXT}}}{\text{Mean } F_{\text{EXT}}}$$

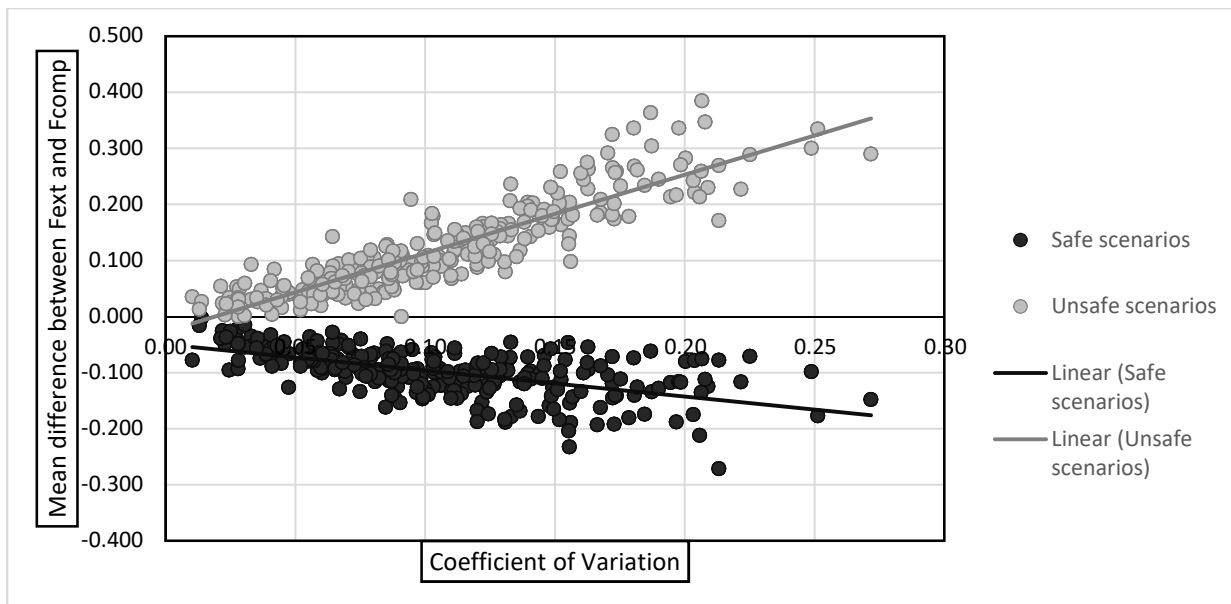


Figure 4.18:  $F_{EXT}$  and  $F_{COMP}$  difference vs coefficient of variation

From analysing the graph in Figure 4.18, it is observed that the difference in factor of safety increases at a faster rate with increased variability for unsafe slope scenarios compared to safe slope scenarios. The mean difference for the unsafe slope scenarios lay between 0 and 0.28 with a maximum difference of 0.385 being observed. For the safe scenarios, the mean difference lay between 0 and -0.15 with a maximum difference of -0.27 being experienced.

On average, for low coefficients of variation of around 0.1, low differences were recorded between  $F_{EXT}$  and  $F_{COMP}$ . Higher differences were recorded for higher coefficients of variations of around 0.2. These findings show that as a slope's level of variability increases, so does the likelihood that an 3D extrapolated slope would provide results that differ from the 3D composite slopes. This is due to an increase in unsafe (i.e. critical) slopes surfaces not be sampled. This results in an increase in the amount of unsafe analyses performed when 3D analyses are done when using 2D extrapolated cross sections.

#### 4.6.2 $F_{2D}$ and $F_{COMP}$ difference vs coefficient of variation graph

A similar graph to that in Figure 4.18 was drawn and can be seen in Figure 4.19. In this case, the mean difference between  $F_{2D}$  and  $F_{COMP}$  values that resulted in safe and unsafe scenarios, for the ideal, average and worst cases, was used. This was plotted against the coefficient of variation of 2D simulation factor of safety results ( $F_{2D}$ ). The coefficient of variation for each set was determined using the formula:

$$\text{Coefficient of variation} = \frac{\text{Standard deviation for } F_{2D}}{\text{Mean } F_{2D}}$$

Additionally, the previous ( $F_{EXT}$ ) trendlines were included in Figure 4.19 for comparative purposes.

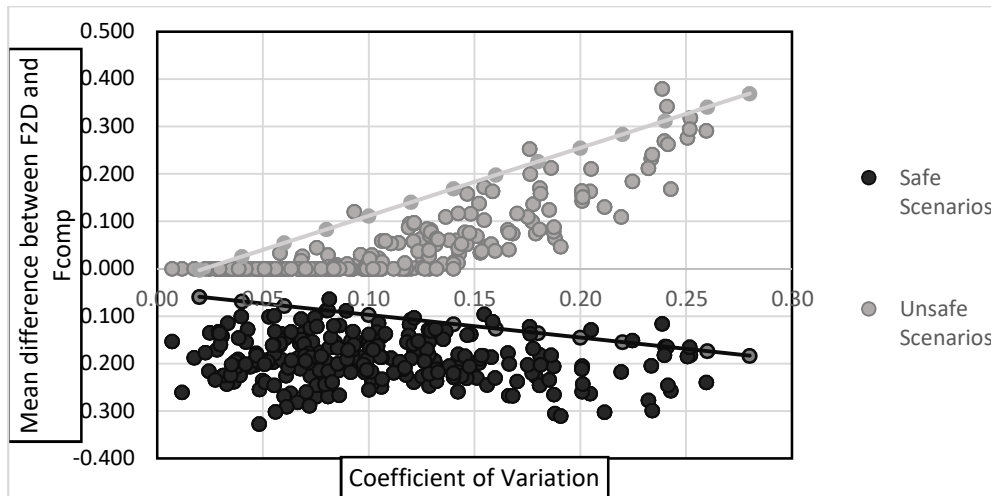


Figure 4.19:  $F_{2D}$  and  $F_{COMP}$  difference vs coefficient of variation graph

From Figure 4.19 it can be seen that for low coefficient of variation values (low spatial variability) of between 0 and 0.07, there are no unsafe analysis results. The maximum difference between  $F_{2D}$  and  $F_{COMP}$  for the unsafe slopes was 0.38 while a maximum difference of -0.33 for the safe slopes. In general, similar to Figure 4.18, for low coefficients of variation of around 0.1, low differences were recorded between  $F_{2D}$  and  $F_{COMP}$ . Higher differences were recorded for higher coefficients of variations of around 0.2.

There are very few unsafe scenarios based on the observation that there are very few points that go above the  $F_{EXT}$  unsafe line (i.e. 4 slopes scenarios) beyond a coefficient of variation value of 0.07. This  $F_{EXT}$  trendline designates the upper bound for the unsafe scenarios formed by the mean difference between  $F_{2D}$  and  $F_{COMP}$ . Similarly, there are very few points which go above the safe trend line which signifies the lower bound for safe scenarios (i.e. 6 slope scenarios). This illustrates the relative safety of carrying out 2D analysis as compared to extrapolating 3D slopes for slope stability analysis.

The results show that when the variability is very low, the possibility of running an unsafe analysis using a 2D method are very low. As variability increases within a slope, so too does the difference between the average  $F_{2D}$  and  $F_{COMP}$  results. This leads to an increase in likelihood that an analysis will yield an unsafe result. However, from comparing the results with the trendlines from Figure 4.18, it is observed that the differences between the average  $F_{2D}$  and  $F_{COMP}$  values do not exceed the differences witnessed between the average  $F_{EXT}$  and  $F_{COMP}$  values. This suggest that 2D analysis is safer than 3D extrapolation methods.

#### 4.6.3 Internal boundary layer comparison for low and high coefficients

It is of interest to observe typical sections which yielded relatively low and high coefficient of variations. Table 4.5 shows typical sections which were obtained from low coefficient of variation values of 0.1 and high coefficient of variation values of 0.2. This was carried out for the different stepped internal boundary layers separating the drained and undrained region i.e. 5m, 3.5m, 2.5m and 1.5m stepped internal boundary layers.

From Figure 4.20 to Figure 4.27 in Table 4.5 the minimum and maximum internal boundaries which resulted in relatively low (0.1) and high (0.2) coefficient of variation values can be observed for the internal boundary thicknesses; 5m, 3.5m, 2.5m and 1.5m. The minimum and maximum boundary originated from a set which was made up of 3 different slopes. Table 4.6 gives the minimum and maximum internal boundary FOS values (i.e.  $F_{2D}$ ,  $F_{EXT}$  and  $F_{COMP}$  values) for the slopes shown in Table 4.5.

The results for the different layers, for both low and high coefficients of variations, show that when the drained region is thick, high factors of safety are calculated. This shows that for slopes with thicker embankment walls, greater stability is experienced. When slopes had thinner embankment walls, lower factors of safety were calculated. This shows how weaker slope conditions are experienced when the embankment walls of a tailings dam are small.

When variability increases, the average difference between  $F_{EXT}$  and  $F_{COMP}$  increases. This increases the probability that an unsafe analysis will be performed. If highly variable conditions are experienced by a slope with thin embankment walls, it is dangerous to perform 3D extrapolation methods.

**Table 4.5: Low versus high spatial variability comparison**

Stepped internal boundary thickness	Coefficient of variation (CoV) = 0.1	Coefficient of variation (CoV) = 0.2
5m	<p>Figure 4.20: Low coefficient of variation for 5m internal layered slope</p>	<p>Figure 4.21: High coefficient of variation for 5m internal layered slope</p>
3.5m	<p>Figure 4.22: Low coefficient of variation for 3.5m internal layered slope</p>	<p>Figure 4.23: High coefficient of variation for 3.5m internal layered slope</p>
2.5m	<p>Figure 4.24: Low coefficient of variation for 2.5m internal layered slope</p>	<p>Figure 4.25: High coefficient of variation for 2.5m internal layered slope</p>
1.5m	<p>Figure 4.26: Low coefficient of variation for 1.5m internal layered slope</p>	<p>Figure 4.27: High low coefficient of variation for 1.5m internal layered slope</p>

**Table 4.6: Low versus high spatial variability comparison table**

	Coefficient of variation (CoV) = 0.1						Coefficient of variation (CoV) = 0.2					
Layer thickness	Min F <sub>2D</sub>	Max F <sub>2D</sub>	Min F <sub>EXT</sub>	Max F <sub>EXT</sub>	Min F <sub>COMP</sub>	Max F <sub>COMP</sub>	Min F <sub>2D</sub>	Max F <sub>2D</sub>	Min F <sub>EXT</sub>	Max F <sub>EXT</sub>	Min F <sub>COMP</sub>	Max F <sub>COMP</sub>
5 m	1.02	1.02	1.11	1.34	1.14	1.18	0.90	1.36	0.95	1.42	1.01	1.04
3.5 m	0.84	1.11	0.95	1.16	1.05	1.08	0.90	1.32	1.05	1.57	1.22	1.26
2.5 m	0.90	1.00	1.06	1.29	1.13	1.37	0.91	1.49	1.05	1.59	1.23	1.42
1.5m	1.24	1.55	1.36	1.6	1.6	1.60	1.24	1.38	1.09	1.60	1.18	1.31

#### 4.7 ANOVA Test

A comparison was conducted on results from the varying stepped placement layer thicknesses inside the slope. This was done in order to find out whether layer thickness had an influence on the slope stability results from the 2D, 3D extrapolated and 3D composite analysis approaches. Table 4.7 below shows a summary of the deterministic factor of safety data obtained from each simulation scenario. In this table, the deterministic factor of safety average values for each scenario were recorded along with their respective standard deviation, coefficient of variation and variance. Table B. 2 to Table B. 4 in the Annexure B also provides the full deterministic, and probabilistic results for the 2D, 3D extrapolated and 3D composite results respectively.

Each simulation scenario contained a different stepped internal boundary geometry separating the drained and undrained region. A single factor ANOVA test was conducted using Excel's statistical software package in order to establish whether the mean deterministic FOS values from the different stepped internal layers boundaries of the slope had a significant relationship. In establishing this, it would become clear on whether layer thickness had an effect on the overall slope stability results for each of the three, slope analysis approach (i.e. 2D, 3D extrapolated and 3D composite).

For each analysis approach, each simulation scenario's mean deterministic FOS values was analysed for the determination of the variance given in Table 4.8. The ANOVA test utilised the variance data in order to determine F-statistic values. The F statistic values were used to assess the equality of means for the different simulation scenarios for each analysis approach. This was done through the determination of p values. Table 4.8 shows the p value results from the single factor ANOVA test produced for the mean FOS data found in Table 4.7. If the p value was lower than the alpha value of 0.05 then, the null hypothesis was rejected, meaning the mean factor of safety values for each layer were statistically different for the analysis approach used. The alpha value indicated the level of significance for the test hypothesis.

From analysing the data in Table 4.8 on the 2D and 3D extrapolated analysis methods, p values higher than 0.05 were obtained. This meant that the mean FOS values recorded for each layer was statistically similar for both analysis approaches. This suggests that layer thickness using these analysis approaches was not an influential factor when it came to the determination of slope analysis results.

.

**Table 4.7: Comparison of layering**

Scenario	Count	2D Deterministic Factor of safety				3D Deterministic Extrapolated Factor of safety				3D Deterministic Composite Factor of safety			
		Average	Standard Deviation	Coefficient of Variation	Variance	Average	Standard Deviation	Coefficient of Variation	Variance	Average	Standard Deviation	Coefficient of Variation	Variance
3 thick (5m)	117	1.15	0,15	0,13	0,023	1,26	0,15	0,12	0,023	1,23	0,10	0,083	0,011
2 thick (5m)	108	1.12	0,16	0,14	0,026	1,24	0,17	0,14	0,029	1,22	0,12	0,10	0,015
3 thick (3.5m)	66	1.12	0,15	0,13	0,021	1,27	0,15	0,12	0,023	1,27	0,12	0,093	0,0140
3 thick (2.5m)	168	1.10	0,13	0,12	0,017	1,28	0,16	0,13	0,027	1,27	0,10	0,083	0,011
4 thick (2.5m)	120	1.11	0,12	0,11	0,016	1,29	0,15	0,12	0,023	1,28	0,11	0,083	0,011
4 thick (1.5m)	171	1.10	0,14	0,13	0,019	1,30	0,15	0,17	0,023	1,29	0,095	0,073	0,0091
5 thick (1.5m)	66	1.11	0,11	0,10	0,013	1,29	0,13	0,099	0,017	1,29	0,089	0,069	0,0079

**Table 4.8: p values**

2D Slopes Factor of safety ( $F_{2D}$ )	3D Extrapolated Slopes Factor of safety ( $F_{EXT}$ )	3D Composite Slopes Factor of safety ( $F_{COMP}$ )
0.166	0.0756	7.5E-11

For 3D composite analysis method, a p value below 0.05 was found. This meant that the null hypothesis could be rejected and indicating that the mean FOS values recorded from each scenario were statistically different. This suggests that the stepped internal layer thickness was an influential factor on the 3D composite FOS results.

What these results suggest is that for the 2D and 3D extrapolated models, the slope stability analyses do not account for the thickness of the internal stepped boundary layers as compared to the more representative 3D composite models. This could be a contributing factor to the inaccuracies that lead to unsafe results being observed when using 2D and 3D extrapolated approaches. However, due to 3D methods often yielding greater FOS values as compared to 2D methods, 3D extrapolated model results are more likely to produce higher and potentially more unsafe FOS values than 2D methods.

#### **4.8 Findings and Practical implications**

The practical implications of the research can now be discussed with relation to tailings dams. It was found that when the strongest section is sampled, within a slope that has a weak arrangement, and analysed using 3D extrapolation procedures, there is a high chance that the slope stability analysis results would be unsafe. This unsafety originates from there being a much more critical section which would have been unsampled, that would yield a much lower and more critical factor of safety. The chances of conducting an unsafe slope stability analysis reduce if a 2D slope stability analysis is conducted. If, however, the weakest section is correctly sampled and extrapolated to conduct 3D slope stability simulations, there is a very low risk of conducting an unsafe slope stability analysis.

For tailings dams which have undergone intensive field investigations with good sampling procedures being implemented, there is a good chance that the weakest section would have been sampled. In such instances, it is safe to use 3D extrapolation techniques to conduct slope stability analysis. However, if little site investigation has been undertaken, then the research suggest that it would be safer to conduct 2D investigations in order to obtain slope stability results. This becomes even more important if the tailings dam has high levels of heterogeneity for instance, due to the presence of multiple internal soil layers with different soil properties.

Furthermore, considerations should be taken on the amount of embankment material on the tailings dam. If a tailings dam has a thick embankment wall, stability is going to be higher than for a tailing with a thin embankment wall. It is thus safer to conduct 3D extrapolated analysis on tailings with thicker walls, provided good sampling and investigation has been conducted.

## Chapter 5: Conclusion and recommendations

The objective of the study was to investigate the risk associated with extrapolating 2D cross sections to carry out 3D slope stability analysis with special reference to tailing dams. From the analysis of the results and the finding, the overall objectives of this research were achieved. This chapter gives the summary of the research findings and conclusions reached

- Of the 816 successful slope stability simulations, a lognormal distribution was observed for the 2D deterministic FOS data, a skewed right distribution was produced from the 3D extrapolated FOS data, and a normal distribution was produced for the 3D composite data.
- It was found that 3D FOS values were higher than the 2D FOS values as proposed in literature. The average percentage difference between the  $F_{2D}$  and  $F_{EXT}$  values was 15%.
- For the ideal-case (i.e. the weakest  $F_{EXT}$  compared to the strongest  $F_{COMP}$ ), 3D extrapolated models yielded unsafe scenarios 1% of the time, whereas 0% of the 2D models were found to be unsafe.
- For the worst-case (i.e. the highest  $F_{EXT}$  compared to the weakest  $F_{COMP}$ ), 3D extrapolated models yielded unsafe cases 99% of the time, whereas 44% of the 2D models were found to be unsafe. This showed that it was safer to conduct 2D slope stability analysis compared to using 3D extrapolated slopes.
- By plotting the average differences between  $F_{EXT}$  and  $F_{COMP}$  values against the coefficient of variation it was found that as heterogeneity increases, so did the average differences between the  $F_{EXT}$  and  $F_{COMP}$  values. This shows that if 3D extrapolated models are used for slopes with high levels of heterogeneity, unsafe results are increasingly obtained.
- By plotting the average difference between  $F_{2D}$  and  $F_{COMP}$  values against the coefficient of variation, it was found that for low levels of heterogeneity, little difference is observed between the  $F_{2D}$  and  $F_{COMP}$  values. However, for high levels of heterogeneity, the difference between the  $F_{2D}$  and  $F_{COMP}$  values increased. This difference however, was not as great as that found for the  $F_{EXT}$  and  $F_{COMP}$  values. This emphasised why 2D analysis methods are safer than 3D extrapolated methods.
- Results also showed that, when the slope embankment walls were thin, lower FOS values were experienced. For slopes with thick embankment walls, higher FOS values were found. This showed that slopes with thicker embankments were more stable as opposed to slopes with thinner embankments. If highly variable conditions are present in a slope with thin embankment walls, it is more dangerous to perform 3D extrapolations.

Overall the research suggests that for tailings dams which have undergone extensive site investigation where there is a good chance that the weakest section would have been sampled, it may be safe to undertake slope stability analysis using 3D extrapolation. However, if there has been limited site investigation the research suggests it is safer to conduct slope stability analysis using 2D methods. This is crucial if the tailings dam has high levels of spatial variability. Therefore, if there is inadequate investigation, it is potentially dangerous to extrapolate 2D cross section to carryout 3D slope stability analysis for tailings dams as this method can exaggerate the factors of safety. Therefore, it is recommended to use 2D slope stability analysis unless there is extensive field investigations.

The following recommendations are made for future studies:

- The use of additional Limit Equilibrium methods is recommended in addition to the Morgenstern and Price, and Spencer's method used in this research. This can be researched with the aim of establishing whether most Limit Equilibrium methods commonly used yield the same outcomes as of those of this research. Possible results which could be found might be the discovery of higher unsafe percentages, as compared to the more rigorous methods used in this research, for the worst-cases.
- This research could also be extended beyond tailings dams to normal earth slopes by comparing the effects of 2D and 3D extrapolated sections, with uniform properties, against 3D realistic models with spatial variable soil properties throughout their entire section. The results of this research could further show that 3D extrapolated sections yield unsafe results compared to 2D slope stability analysis when compared to more realistic 3D model results.
- An automated approach could be implemented by using a programmable slope stability generation system. This would allow for more slope stability analysis simulations to be performed which would allow for more results to be obtained. This would allow for more probability of failure data to be acquired during the probabilistic analysis. In doing this, further comparisons could be done which substantiate 3D extrapolated models being unsafe as compared to 2D slope stability methods.

## References

1. Aghajani, H.F., Salehzadeh, H. & Shahnazari, H. 2015. Stability analysis of sandy slope considering anisotropy effect in friction angle. *Sadhana - Academy Proceedings in Engineering Sciences*. 40(6):1955–1974. Available: <https://www.ias.ac.in/article/fulltext/sadh/040/06/1955-1974>
2. Akhtar, K. 2011. *Three-Dimensional Slope Stability Analyses for Natural and Manmade Slopes*. Published doctoral dissertation. Ann Arbor: ProQuest.
3. Albataineh, N. 2006. Slope Stability Analysis using 2D and 3D Methods. Published master's thesis. Ohio: University of Akron.
4. Allan, F.C., Yacoub, T.E. & Curran, J.H. 2012. Using Spatial Methods for Heterogeneous Slope Stability Analysis. *46th US Rock Mechanics/Geomechanics Symposium*. OnePetro.
5. Atkinson, J. 2007. *The Mechanics of Soils and Foundations Second Edition*. New York: Taylor and Francis.
6. Australian National Committee on Large Dams (ANCOLD). 2012. *Guidelines on Tailings Dams: Planning, Design, Construction, Operation and Closure*. Available: <https://www.resolutionminees.us/sites/default/files/references/ancold-2012.pdf> [2021, May 19].
7. Azami, A., Yacoub, T., & Curran, J. H. (2012). Effects of strength anisotropy on the stability of slopes. *65<sup>th</sup> Canadian Geotechnical Conference, Geo-Manitoba*. 1 September, Toronto.
8. Bhanbhro, R. (2017). *Mechanical Behavior of Tailings Laboratory: Tests from a Swedish Tailings Dam*. Published doctoral thesis. Sweden: Lulea University of Technology [Online]. Available: <https://doi.org/10.13140/RG.2.2.29809.68969>
9. Blight, G. E., and Bentel, G. M. (1983). "The behaviour of mine tailings during hydraulic deposition. *Journal of the Southern African Institute of Mining and Metallurgy*, 83(4), 87-91. Available: [https://journals.co.za/doi/10.10520/AJA0038223X\\_1377](https://journals.co.za/doi/10.10520/AJA0038223X_1377)
10. Blight, G. E., Thomson, R. R., and Vorster, K. (1985). "Profiles of hydraulic-fill tailings beaches, and seepage through hydraulically sorted tailings. *Journal of the South African Institute of Mining and Metallurgy*, 85(5), 157-161. Available: [https://journals.co.za/doi/abs/10.10520/AJA0038223X\\_1961](https://journals.co.za/doi/abs/10.10520/AJA0038223X_1961)
11. Budhu, M. 2011. *Soil Mechanics and Foundations (3rd Edition)*. John Wiley.
12. Chakraborty, A. & Goswami, D. 2018. Three-dimensional (3D) slope stability analysis using stability charts. *International Journal of Geotechnical Engineering*. 15(5):642–649.

13. Chatterjee, D. & Murali Krishna, A. 2021. Stability analysis of two-layered non-homogeneous slopes. *International Journal of Geotechnical Engineering*. 15(5):16–26.
14. Chaudhary, K.B., Fredlund, M. & Lu, H. 2016. *Three-Dimensional Slope Stability: Geometry Effects*. Canada: Soil Vision Systems Ltd.
15. Duncan, J.M., Wright, S.G., Brandon, T. L. 2014. *Soil Strength and Slope Stability 2nd Edition*. New Jersey: John Wiley.
16. Huang, C., Tsai, C. & Chen, Y. 2002. Generalized method for three-dimensional slope stability analysis. *Journal of geotechnical and geoenvironmental engineering*, 128(10): 836-848. Available: [https://ascelibrary.org/doi/abs/10.1061/\(ASCE\)1090-0241\(2002\)128:10\(836\)](https://ascelibrary.org/doi/abs/10.1061/(ASCE)1090-0241(2002)128:10(836))
17. Hicks, M.A. & Spencer, W.A. 2009. Influence of heterogeneity on the reliability and failure of a long 3D slope. *Computers and Geotechnics*. 37(7–8):948–955. Available: <https://doi.org/10.1016/j.compgeo.2010.08.001>
18. Hicks, M.A., Nuttall, J.D. & Chen, J. 2014. Influence of heterogeneity on 3d slope reliability and failure. *Computers and Geotechnics*. 61(2014):198–208. Available: <https://doi.org/10.1016/j.compgeo.2014.05.004>
19. Hwang, J., Dewoolkar, M. & Ko, H.Y. 2002. Stability analysis of two-dimensional excavated slopes considering strength anisotropy. *Canadian Geotechnical Journal*. 39(5):1026–1038. Available: <https://doi.org/10.1139/t02-057>
20. ICOLD. (2020). *Tailings dam safety*. Committee L Tailings Dams and Waste Lagoons. Available: <https://www.spancold.org/wp-content/uploads/2021/02/JSPEM20210223-Tailings-Dam-Safety-Bulletin-Francisco-S%C3%A1nchez.pdf> [2021, July 25].
21. Kalatehjari, R. & Ali, N. 2013. A review of three-dimensional slope stability analyses based on limit equilibrium method. *Electronic Journal of Geotechnical Engineering*. 18: 119–134. Available: [https://www.researchgate.net/publication/236174492\\_A\\_Review\\_of\\_Three-Dimensional\\_Slope\\_Stability\\_Analyses\\_based\\_on\\_Limit\\_Equilibrium\\_Method](https://www.researchgate.net/publication/236174492_A_Review_of_Three-Dimensional_Slope_Stability_Analyses_based_on_Limit_Equilibrium_Method)
22. Malkawi, A.I.H., Hassan, W.F. & Sarma, S.K. 2001. Global Search Method for Locating General Slip Surface Using Monte Carlo Techniques. *Journal of Geotechnical and Geoenvironmental Engineering*. 127(8):688–698. Available: [https://ascelibrary.org/doi/abs/10.1061/\(ASCE\)1090-0241\(2001\)127:8\(688\)](https://ascelibrary.org/doi/abs/10.1061/(ASCE)1090-0241(2001)127:8(688))
23. MacRobert, C. J., and Blight, G. E. 2013. A field study of the in situ moisture regime during active hydraulic tailings deposition. *Journal of the South African Institution of Civil Engineering*, 55(3), 57-68. Available: <https://journals.co.za/doi/10.10520/EJC152559>
24. Menčík, J. 2016. *Concise Reliability for Engineers*. Rijeka: Intech

25. Pan, H., Cheng, Z., Zhou, G., Yang, R., Sun, B., He, L., Zeng, D. and Wang, J. 2017. Geochemical and mineralogical characterization of tailings of the Dexing copper mine, Jiangxi Province, China. *Geochemistry: Exploration, Environment, Analysis*, 17(4): 334-344. Available: <https://sci-hub.ee/10.1144/geochem2016-457>
26. Ranjan, G. and Rao, A.S.R. (2000). *Basic and Applied Soil Mechanics*. New Age International Publisher, New Delhi, India.
27. Robertson, P.K. & Cabal (Robertson), K.L. 2012. *Guide to Cone Penetration Testing for Geotechnical Engineering*. California: Gregg.
28. Rocscience, 2021. *Correlation length* [Online]. Available: [https://www.rocscience.com/help/slide2/slide\\_model/probability/spatial\\_variability.htm](https://www.rocscience.com/help/slide2/slide_model/probability/spatial_variability.htm) [2021, May 25].
29. Rocscience, 2021. *Cuckoo Search* [Online]. Available: [https://www.rocscience.com/help/slide2/slide\\_model/surfaces/cuckoo\\_search.htm](https://www.rocscience.com/help/slide2/slide_model/surfaces/cuckoo_search.htm) [2021, May 25].
30. Rocscience, 2021. *Auto Refine Search* [Online]. Available: [https://www.rocscience.com/help/slide2/slide\\_model/surfaces/auto\\_refine\\_search\\_non-circular.htm](https://www.rocscience.com/help/slide2/slide_model/surfaces/auto_refine_search_non-circular.htm) [2021, May 25].
31. Shehata, H., Desai, C. S., & Congress, I. 2018. *Advances in numerical methods in geotechnical engineering*. Egypt: Springer
32. Su, S.F. & Liao, H.J. 1999. Effect of strength anisotropy on undrained slope stability in clay. *Geotechnique*. 49(2):215–230. Available: <https://doi.org/10.1680/geot.1999.49.2.215>
33. Stark, T. D. & Ruffing, D.G. 2017. Selecting Minimum Factors of Safety for 3D Slope Stability Analyses. *Geo-Risk 2017*. 259–266. Available: <https://ascelibrary.org/doi/abs/10.1061/9780784480700.025>
34. The Mining Association of Canada (MAC). 2019. *A Guide to the Management of Tailings Facilities Version 3.1*[Online]. Available: <https://mining.ca/documents/a-guide-to-the-management-of-tailings-facilities-version-3-1-2019/> [2018, March 18].
35. Thi Minh Hue Le, Domenico Gallipoli, Marcelo Sanchez, S.W. 2014. Stability and Failure Mass of Unsaturated Heterogeneous Slopes. *Canadian Geotechnical Journal*. 44(0):1–56
36. Varkey, D., Hicks, M.A. & Vardon, P.J. 2017. Influence of Spatial Variability of Shear Strength Parameters on 3D Slope Reliability and Comparison of Analysis Methods. *Geo-Risk 2017 GSP*. 400–409.

37. Vick, S.G. 1990. *Design, and Analysis of Tailings Dams*. Vancouver: BiTech Publishers Ltd
38. Walck, C 2007. *Handbook on Statistical Distributions for experimentalists*. Stockholm: University of Stockholm.
39. Whitlow, R. 1995. *Basic Soil Mechanics (3rd edition)*. Bristol: Longman.
40. Wei, Z., Yin, G., Wan, L. & Li, G. 2016. A case study on a geotechnical investigation of drainage methods for heightening a tailings dam. *Environmental Earth Sciences*. 75(2):106. Available: <https://link.springer.com/content/pdf/10.1007/s12665-015-5029-8.pdf>

## Annexure: A

**Table A. 1: Excel Data record guide**

<b>First level data</b>	
<b>Master Full (Recorded simulation data):</b> In this excel file, the full 1032 recorded simulation results are found	
<b>Second level data</b>	
<b>Master Full (Abnormal surfaces removed):</b> In this excel file, the 816 recorded simulation results are found with the erroneous surfaces marked off.	
<b>Third level data</b>	
<b>Master Analysis Full:</b> In this Excel file the full analysis of the recorded results can be found	

Phoon and Kulhawy 1999				Shen 2012 (Thesis)	
Property	Soil Type	Mean	Std. Dev./Mean	Property	Std. Dev./Mean
Undrained Cohesion(UC)	clay	10 - 400 kN/m <sup>2</sup>	0.2 - 0.55	Undrained Cohesion	13 - 40
Undrained Cohesion(UU)	clay	10 - 350 kN/m <sup>2</sup>	0.1 - 0.3	Unit Weight	3 - 7
Undrained Cohesion(CIUC)	clay	10 - 400 kN/m <sup>2</sup>	0.2 - 0.4	Bulk Unit Weight	0 - 10
Friction Angle	clay and sand	20 - 40 °	0.05 - 0.15	Friction Angle	2 - 13
Undrained Cohesion(VST)	clay	5 - 400 kN/m <sup>2</sup>	0.1 - 0.4		
Unit Weight	clay and silt	13 - 20 kN/m <sup>3</sup>	< 0.1		

Figure A. 1: RocScience recommended material statistics (Slide 2 & Slide 3)

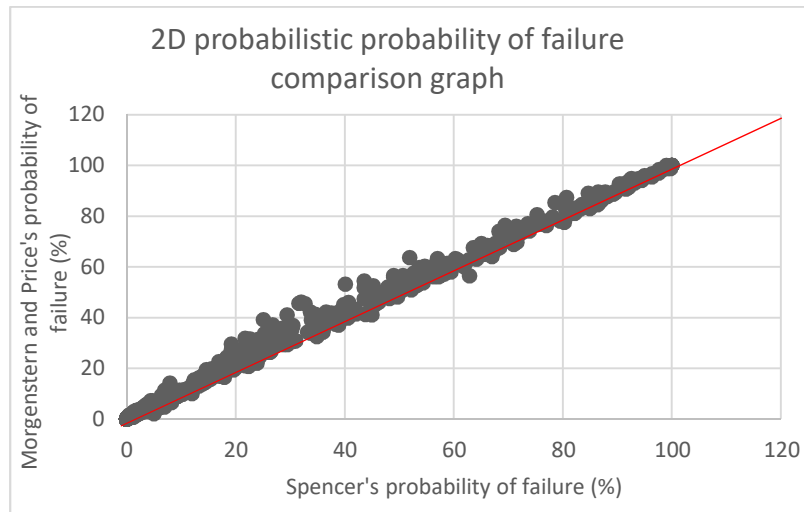


Figure A. 2: 2D probabilistic probability of failure comparison graph

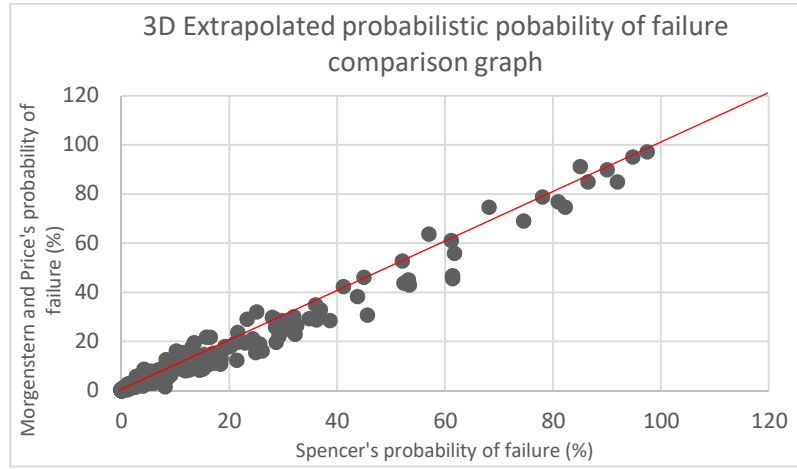


Figure A. 3: 3D extrapolated probabilistic probability of failure comparison graph

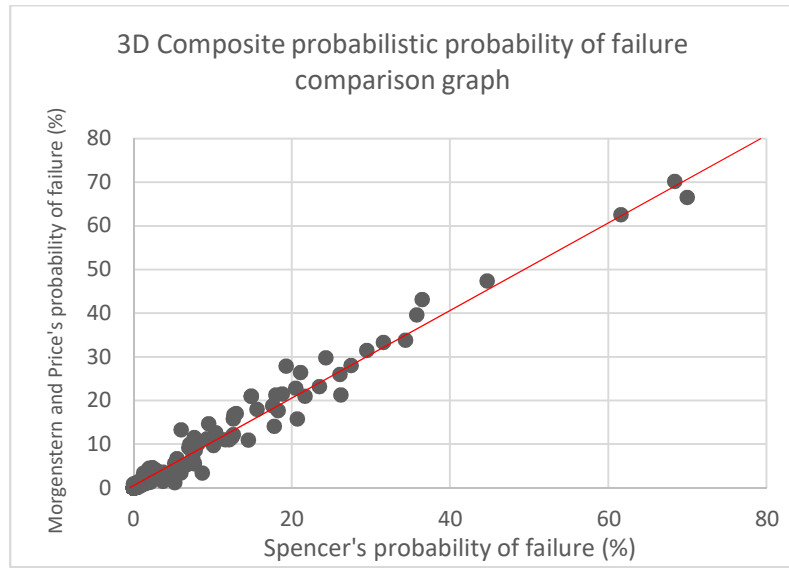


Figure A. 4: 3D composite probabilistic probability of failure comparison graph

## Annexure B

### Result records

The *Master (Recorded Simulation data)* Excel spread-sheet, gives the recorded results outputted during the simulations of the Research. Inside the spread-sheet, different scenarios are provided with different slopes with their analysis results. Table B. 1 gives the list of the different scenarios.

**Table B. 1: Simulation scenarios**

Scenario	Name
1	3 thick (5m)
2	2 thick (5m)
3	3 thick (2.5m)
4	4 thick (2.5m)
5	4 thick (1.5m)
6	5 thick (1.5m)
7	3 thick (3.5m)

### Slope Stability Analysis Sample Results

The slide software did not have input and an output file hence a convenient format of recording all three types of simulations was developed. The outer geometry was present at every simulation accompanied by the internal boundary coordinates. Alongside the internal boundary coordinates, the barcode and the results for Morgenstern and Price; and Spencer's Method are given. Typical illustrations of these output results are shown in Figure B. 1 and Figure B. 2

### Morgenstern and Price method Sample results

Figure B. 1 shows the results from the Morgenstern and Price method. The figure shows the Slope's outer geometry coordinates; the internal boundary coordinates between the undrained region and the drained region. Figure 4.1 also shows the results for the deterministic factor of safety, the probabilistic factor of safety and probability of failure for the three scenarios: 2D, 3D Extrapolated (Extruded) and 3D Composite using the Morgenstern and Price method.

Set 1			
Run 1			
Outer Geometry		Inside	
X	Z	Inside	12
0	0	Inside geometry	
150	0	X	Z
90	30		50 30
0	30		50 25
0	0		45 25
			45 20
			55 20
			55 15
			65 15
			65 10
			115 10
			115 5
			120 5
			120 0
Barcode		5050454555556565115115120120	302525202015151010550

2D Results		Morgenstern and Price	123	3D composite results	Morgenstern and Price
Deterministic Factor of safety		1.089		Deterministic Factor of safety	1.203
Probabilistic factor of safety		1.089		Probabilistic factor of safety	1.208
Probability of failure		8.4		Probability of failure	0.1
3D Extruded Results					
Deterministic Factor of safety		1.202			
Probabilistic factor of safety		1.201			
Probability of failure		0.1			

Figure B. 1: Sample Record book illustration for Morgenstern and Price

### Spencer Method sample results

Similarly, Figure B. 2 shows the results from the Spencer method. Similar to Figure B. 1, the figure gives the Slope's outer geometry coordinates; the internal boundary coordinates between the undrained region and the drained region. The results for the deterministic factor of safety, the probabilistic factor of safety and probability of failure for the three scenarios: 2D, 3D Extrapolated (Extruded) and 3D Composite using the Spencer's Method are shown.

Set 1			
Run 1			
Outer Geometry		Inside	
X	Z	Inside	12
0	0	Inside geometry	
150	0	X	Z
90	30		50 30
0	30		50 25
0	0		45 25
			45 20
			55 20
			55 15
			65 15
			65 10
			115 10
			115 5
			120 5
			120 0
Barcode		5050454555556565115115120120	302525202015151010550

2D Results		Spencer	123	3D composite results	Spencer
Deterministic Factor of safety		1.089		Deterministic Factor of safety	1.196
Probabilistic factor of safety		1.089		Probabilistic factor of safety	1.204
Probability of failure		8.8		Probability of failure	0.2
3D Extruded Results					
Deterministic Factor of safety		1.171			
Probabilistic factor of safety		1.178			
Probability of failure		0.3			

Figure B. 2: Record book illustration of Results from Spencer Method

Bar codes are placed under every simulation in order to ensure the uniqueness of each slope stability surface analysed and prevent repetitions.

*Figure B. 3: Typical abnormal section*

**Table B. 2: 2D slope analysis average data based on internal boundary thickness**

Scenario	Count	Factor of safety				Average Probabilistic Factor of safety				Probability of failure			
		Average	Standard Deviation	Coefficient of Variation	Variance	Average	Standard Deviation	Coefficient of Variation	Variance	Average	Standard Deviation	Coefficient of Variation	Variance
3 thick (5m)	117	1,15	0,15	0,13	0,023	1,15	0,15	0,13	0,023	18,19	27,47	1,51	754,86
2 thick (5m)	108	1,12	0,16	0,14	0,026	1,12	0,16	0,14	0,026	28,39	34,92	1,23	1219,68
3 thick (2,5m)	168	1,12	0,15	0,13	0,021	1,12	0,15	0,13	0,022	25,04	35,74	1,43	1277,37
4 thick (2,5m)	120	1,10	0,13	0,12	0,017	1,10	0,13	0,12	0,017	27,04	32,51	1,20	1056,88
3 thick (3,5m)	66	1,11	0,12	0,11	0,016	1,11	0,13	0,11	0,016	22,37	28,69	1,28	823,13
4 thick (1,5m)	171	1,10	0,14	0,13	0,019	1,10	0,14	0,13	0,019	27,84	29,65	1,07	879,07
5 thick (1,5m)	66	1,11	0,11	0,10	0,013	1,11	0,11	0,10	0,013	20,37	23,22	1,14	538,95

**Table B. 3: 3D Extrapolated slope analysis average data based on internal boundary thickness**

Scenario	Count	Factor of safety				Average Probabilistic Factor of safety				Probability of failure			
		Average	Standard Deviation	Coefficient of Variation	Variance	Average	Standard Deviation	Coefficient of Variation	Variance	Average	Standard Deviation	Coefficient of Variation	Variance
3 thick (5m)	117	1,26	0,15	0,12	0,023	1,27	0,15	0,12	0,023	4,38	13,23	3,02	174,93
2 thick (5m)	108	1,24	0,17	0,14	0,029	1,24	0,17	0,14	0,030	9,81	22,42	2,29	502,79
3 thick (2.5m)	168	1,28	0,16	0,13	0,027	1,28	0,16	0,13	0,027	4,58	12,17	2,66	148,04
4 thick (2.5m)	120	1,29	0,15	0,12	0,023	1,29	0,15	0,12	0,023	2,49	6,25	2,51	39,05
3 thick (3.5m)	66	1,27	0,15	0,12	0,023	1,27	0,15	0,12	0,023	4,13	12,06	2,92	145,47
4 thick (1.5m)	171	1.3	0.15	0.12	0.023	1.3	0.15	0.12	0.023	1.36	3.98	2.91	15.82
5 thick (1.5m)	66	1.29	0.13	0.1	0.017	1.3	0.13	0.1	0.016	0.67	1.97	2.93	3.88

**Table B. 4: 3D Composite slope analysis average data based on internal boundary thickness**

Scenario	Count	Factor of safety				Average Probabilistic Factor of safety				Probability of failure			
		Average	Standard Deviation	Coefficient of Variation	Variance	Average	Standard Deviation	Coefficient of Variation	Variance	Average	Standard Deviation	Coefficient of Variation	Variance
3 thick (5m)	117	1,23	0,10	0,08	0,011	1,23	0,10	0,08	0,011	1,97	6,23	3,17	38,85
2 thick (5m)	108	1,22	0,12	0,10	0,015	1,22	0,12	0,10	0,015	5,21	12,10	2,32	146,37
3 thick (2,5m)	168	1,27	0,11	0,08	0,011	1,27	0,11	0,08	0,011	1,24	3,72	2,99	100,55
4 thick (2,5m)	120	1,27	0,12	0,09	0,014	1,27	0,12	0,09	0,014	2,47	10,03	4,07	0,47
3 thick (3,5m)	66	1,28	0,11	0,08	0,011	1,29	0,11	0,08	0,012	0,77	3,65	4,75	13,85
4 thick (1,5m)	171	1,29	0,10	0,07	0,009	1,30	0,10	0,07	0,009	0,19	0,73	3,85	13,30
5 thick (1,5m)	66	1,29	0,09	0,07	0,008	1,30	0,09	0,07	0,008	0,21	0,68	3,19	0,54

## Annexure C

This section contains explanations of key terminologies and concepts which were mentioned in the research.

### Terminology

#### Correlation length

According to the Rocscience, correlation length represents the distance between which two soil particles having similar properties. This can be related to the field by determining the soil properties of soils at different locations. As the locations of testing increase (i.e. two samples are tested further and further apart), there becomes a tendency for the properties to become different. When a large correlation length is used, it means the soil's spatial variability changes gradually over distance. Small correlation lengths mean the spatial variability of the soil occurs frequently over a short distance. Slopes with small correlation lengths have a behaviour which is much more unpredictable hence it is more important to analyse the slopes probabilistically due to many uncertainties (Rocscience, 2021).

Correlation length can be experienced both horizontally and vertically. If more horizontal correlation lengths are equal the vertical correlation lengths, the more the soils are regarded as isotropic (Rocscience, 2021). In the field cases, it is often observed that variability in the vertical direction occurs more frequently than it is in the horizontal direction. This is due to the vertical direction having smaller correlation length (Rocscience, 2021).

### Statistical Distributions

#### Normal distribution

Normal distributions also known as a Gaussian distribution are regarded as the most common probability distribution due to their behaviour of mimicking many natural occurrences. The distribution is symmetrical with the highest peak, while the values at both sides decreases gradually as the distances from the centre increases, similar to a bell shape (Walck, 2007). The probability distribution function for this distribution is as follows

$$f(x) = \frac{1}{\sigma\sqrt{2\pi}} e^{-\frac{(x-\mu)^2}{2\sigma^2}}$$

- $x$  = random value
- $\mu$  = mean
- $\sigma$  = standard deviation

### **Lognormal distribution**

Lognormal distribution can be summarised as the distribution of logarithmic values which are related to a normal distribution. This distribution is normally suitable for skewed distributions which have a low mean and a high variance, which measures the variability from the data average, within the data set (Walck, 2007). In general, all positive values follow this distribution. The probability distribution function is as follows

$$f(x) = \frac{1}{\sigma\sqrt{2\pi}} e^{-\frac{(\ln x - \mu)^2}{2\sigma^2}}, \quad x > 0$$

- $x$  = random value
- $\mu$  = mean
- $\sigma$  = standard deviation

### **Statistical sampling methods**

In order to simulate random variables, statistical sampling methods have been used. A large number of random sampling is generated to find larger and more desirable properties of the system. The Monte Carlo is normally the standard method used for sampling Random data; however, the Latin Hypercube, which at times gives better results as compared to the Monte Carlo simulation, is also used.

#### I) Monte Carlo Simulation

Monte Carlo simulation creates an arbitrary test of  $N$  points for each uncertain input variable of demonstration. It picks each point for that input variable independently from the probability transmission (Menčík, 2016). It generates a test of  $N$  values for each outcome variable in the demonstration, employing each of the comparing  $N$  points for each ambiguous input. It estimates statistical parameters such as the mean and standard deviation for each outcome based on this arbitrary test (Menčík, 2016).

## II) Latin Hypercube

The Latin Hypercube is another means of random sampling which at times gives arguably better results as compared to the Monte Carlo simulation. This is because the Monte Carlo simulation requires a lot of numbers to create the simulations before convergence occurs. The Latin Hypercube is used to get a good representation of probability distribution, as compared to Monte Carlo were new samples are generated without considering the previously sampled points. Latin Hypercube simulation is dependent on previously sampled data. It involves the equal subdivision of cumulative density functions before choosing random data in each subdivision (Menčík, 2016). With this method, a better representation of the expected distribution is acquired when receiving the output parameters. This makes it especially suitable for slope stability spatial variable analysis cases.